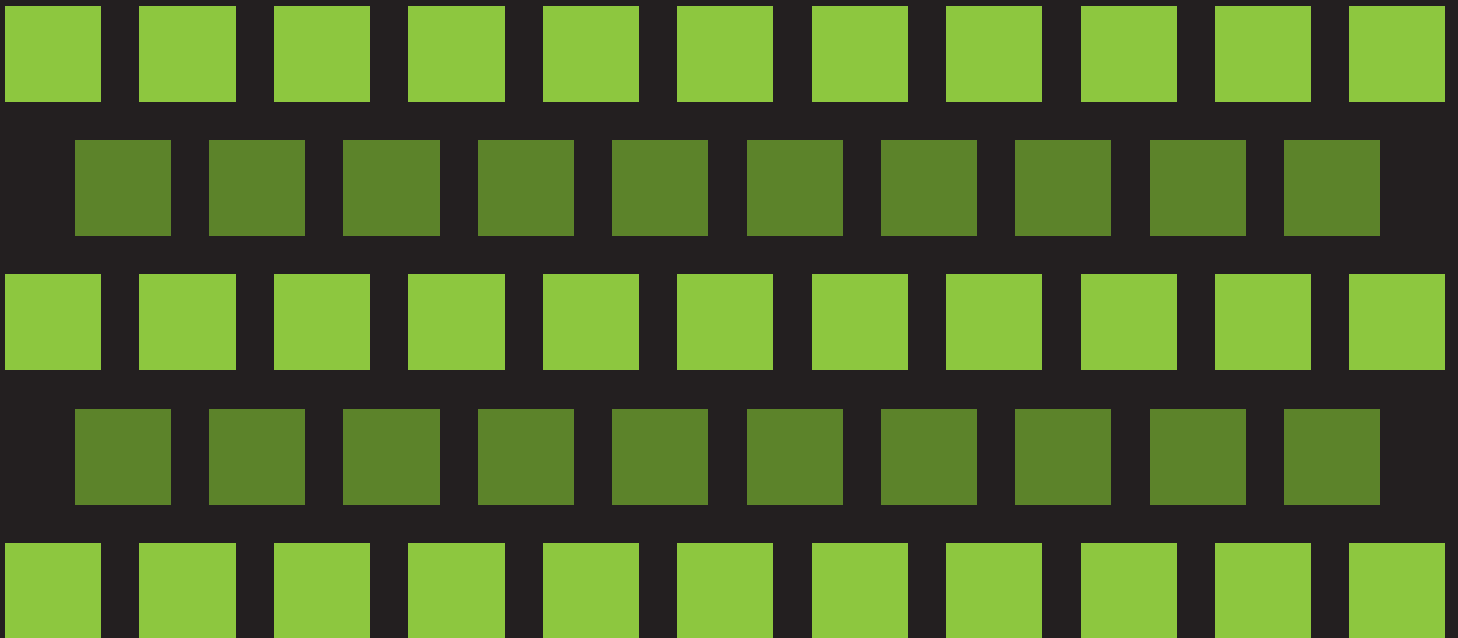


EXTEND STRESS-STRAIN CURVE PARAMETERS AND CYCLIC STRESS-STRAIN CURVES TO ALL MATERIALS LISTED FOR SECTION VIII, DIVISIONS 1 AND 2 CONSTRUCTION



STP-PT-056

**EXTEND STRESS-STRAIN
CURVE PARAMETERS AND
CYCLIC STRESS-STRAIN
CURVES TO ALL MATERIALS
LISTED FOR SECTION VIII,
DIVISIONS 1 AND 2
CONSTRUCTION**

Prepared by:

Wolfgang Hoffelner
RWH consult GmbH



Date of Issuance: April 5, 2013

This report was prepared as an account of work sponsored by ASME Pressure Technology Codes & Standards and the ASME Standards Technology, LLC (ASME ST-LLC).

Neither ASME, ASME ST-LLC, the author, nor others involved in the preparation or review of this report, nor any of their respective employees, members or persons acting on their behalf, makes any warranty, express or implied, or assumes any legal liability or responsibility for the accuracy, completeness or usefulness of any information, apparatus, product or process disclosed, or represents that its use would not infringe upon privately owned rights.

Reference herein to any specific commercial product, process or service by trade name, trademark, manufacturer or otherwise does not necessarily constitute or imply its endorsement, recommendation or favoring by ASME ST-LLC or others involved in the preparation or review of this report, or any agency thereof. The views and opinions of the authors, contributors and reviewers of the report expressed herein do not necessarily reflect those of ASME ST-LLC or others involved in the preparation or review of this report, or any agency thereof.

ASME ST-LLC does not take any position with respect to the validity of any patent rights asserted in connection with any items mentioned in this document, and does not undertake to insure anyone utilizing a publication against liability for infringement of any applicable Letters Patent, nor assumes any such liability. Users of a publication are expressly advised that determination of the validity of any such patent rights, and the risk of infringement of such rights, is entirely their own responsibility.

Participation by federal agency representative(s) or person(s) affiliated with industry is not to be interpreted as government or industry endorsement of this publication.

ASME is the registered trademark of the American Society of Mechanical Engineers.

No part of this document may be reproduced in any form,
in an electronic retrieval system or otherwise,
without the prior written permission of the publisher.

ASME Standards Technology, LLC
Two Park Avenue, New York, NY 10016-5990

ISBN No. 978-0-7918-6883-6

Copyright © 2013 by
ASME Standards Technology, LLC
All Rights Reserved

TABLE OF CONTENTS

Foreword	vi
Executive Summary	vii
1 INTRODUCTION	1
2 METHODS OF PARAMETERIZATION OF STRESS-STRAIN CURVES	3
2.1 Engineering Stress-Strain Curves.....	3
2.2 True Stress-Strain Curves.....	6
3 THE DILEMMA OF FINDING THE (USUALLY NOT AVAILABLE) ULTIMATE TENSILE STRAIN.....	13
3.1 Rasmussen Procedure.....	13
3.2 The MPC-approach	13
3.3 The UTS-YS Approach.....	15
4 CRITICAL ASSESSMENT OF THE DIFFERENT APPROACHES USING ACTUAL STRESS-STRAIN CURVES.....	19
4.1 Carbon Steels.....	19
4.2 Ferritic Steels.....	22
4.3 Martensitic Steels	22
4.4 Austenitic Steels.....	22
4.5 Gamma Prime Hardening Superalloys	23
4.6 Other Classes of Materials	23
5 TANGENT MODULUS	24
6 CYCLIC STRESS-STRAIN CURVES	26
7 PROPOSAL FOR IMPLEMENTATION OF STRESS-STRAIN CURVES INTO THE ASME CODE.....	32
8 REFERENCES	35
Appendix A – Determination of the stress-strain curve using two data points	37
Appendix B – Comparison for IN 800H (rational polynomial, ASME II, Ramberg-Osgood)	40
Appendix C – Data-sheets (true stress-strain curves, modulus) for cross comparison.....	44
Appendix D – Excel map which calculates stress-strain curves and tangent moduli according to MPC and RO-eng.....	51
Acknowledgments.....	52

LIST OF TABLES

Table 1—Parameters for Ultimate Tensile Strain (m_2) and for Start of Plastic Deformation (ϵ_p) for Different Classes of Materials as Defined in the MPC ASME VIII/2 Procedure	14
Table 2—Measured Ultimate Tensile and Yield Stresses	17

LIST OF FIGURES

Figure 1—Engineering and True Stress-strain Curves for 316 Measured at Room Temperature	4
Figure 2—Engineering Stress vs. Engineering Plastic Strain for 316 Measured at Room Temperature	5
Figure 3—True Stress vs. True Plastic Strain for 316 Measured at Room Temperature.....	5
Figure 4—Shape of $(1+\tanh\psi(H))$ and $(1-\tanh\psi(H))$ for 304 L Stainless Steel at Room Temperature	8
Figure 5—Comparison of Different Parameterizations of a True Stress-strain Curve for an Austenitic Steel at Room Temperature	9
Figure 6—Comparison of a Modified MPC True Stress-strain Curve (Equal Slope) with the Other Stress-strain curve parameterizations shown in Figures 4 and 5	10
Figure 7—Comparison of Results from MPC and RO-eng Results Omitting Data-points at the Transition from Low Strain to High Strain for the MPC Approach	11
Figure 8—Comparison of Different True Stress-strain Parameterizations.....	11
Figure 9—Correlation between Yield Stress, Ultimate Tensile Stress and Ultimate Tensile Strain (replotted from Rasmussen [16])	13
Figure 10—Ultimate Tensile Strains Determined According to Table 1 for Different Classes of Materials as Function of Ratio between Yield Stress and Ultimate Tensile Stress	14
Figure 11—Comparison of Predicted and Measured Ultimate Tensile Strains Experimental Data Exclusively from [1]	15
Figure 12—Experimentally Determined Ultimate Tensile Strains (see Table 1) as a Function of the Differences between Ultimate Tensile Stress and Yield Stress	16
Figure 13—Comparison between Calculated and Measured Ultimate Tensile Strains.....	16
Figure 14—Comparison of RO-eng and MPC Curves as Calculated (a) and Using the Actually Measured Ultimate Tensile Strain (b).....	18
Figure 15—Stress-strain Curves of Different Carbon Steels [17]	20
Figure 16—Stress-strain Curves for SA-36 Determined According to MPC and RO-eng Procedures without Lueders Strain Corrections.....	20
Figure 17—Comparison of Results from MPC and RO-eng Parameterizations of A514 (see Figure 15) with the Result from the Lueders-modified RO Approach (RO-eng_lueders).....	21
Figure 18—Stress-strain Curve of a Carbon Steel Without Occurrence of Lueders Strain.....	21
Figure 19—Occurrence of Secondary Hardening for Austenitic Steel at Temperatures below Room Temperature [18].....	22
Figure 20—Comparison of Measured and Calculated Stress-strain Curves of IN-718 at Room Temperature	23
Figure 21—Scheme for Determination of the Tangent Modulus According to the MPC Procedure Described in Section VIII/2	24
Figure 22—Comparison of Tangent Moduli Determined According to the MPC and to the RO-eng Procedure (Materials 2.25Cr-1Mo, RT).....	25

Figure 23—Cyclic Response of a Ti-containing Austenitic Steel at 650°C in 20% Cold Worked and in Annealed Condition [21]	26
Figure 24—Comparison of Cyclic Stress-strain Curves for 304 at Room Temperature.....	27
Figure 25—Experimental Results from LCF-tests of the Austenitic Steel 316LN in Annealed Condition [20]	28
Figure 26—Comparison of a Measured Cyclic Stress-strain Curve (b) with a Cyclic Stress-strain Curve Determined only from Two Data Points (a) Given in [20].....	28
Figure 27—Proposal for Scaling of Cyclic Stress-strain Curve when Different Monotonic Curves Exist.....	28
Figure 28—Monotonic and Cyclic Stress-strain Curves for Different Classes of SA-723 as Derived from Literature.....	29
Figure 29—Cyclic and Monotonic Stress-strain Curves of 17-4 PH in Two Different Qualities.....	30
Figure 30—Cyclic and Monotonic Stress-strain Curves of Grade 91 Martensitic Steel According to the Japanese NIMS [25] Database and the ASME Code.....	30
Figure 31—Comparison of Cyclic and Monotonic Stress-strain Curves for Grade 91 in Current Code Edition.....	31
Figure 32—Consideré Plot for the Determination of the Maximum Stress (UTS).....	38
Figure 33—Comparison of the Polynomial Fit with a YS and UTS Based Power Law Fit	40
Figure 34—Comparison of Different Parameterizations of Stress-strain Curves Applied to IN 800H Determined at 1100F	40
Figure 35—Isochronous Stress-strain Curves from the German KTA	41
Figure 36—Identification of the Points Taken for Digitization of the KTA Stress-strain Curve	41
Figure 37—Comparison of YS-UTS Based Power Law Fit with KTA-data at Low Strains.....	42
Figure 38—Comparison of YS-UTS Based Power Law Fit with KTA-data at High Strains	42
Figure 39—Plastic Strains for the Stress-Strain Curves Determined in KTA.....	43
Figure 40—Comparison of Plastic Strains Taken from Figure 39 with the Ones Determined with the Power Law Fit Procedure	43

FOREWORD

Different approaches currently exist in the ASME code for the determination of monotonic stress-strain curves. ASME Section VIII Div. 2 and FFS-1 use predominantly a two power law approach based on Y-1 and U-table values for direct prediction of true stress-strain curves. Sometimes, also a single power law approach for direct determination of true stress strain curves is used. Section III uses a rational polynomial for determination of isochronous stress strain curves. The report evaluates capabilities and limitations of the different methods using experimental results from literature and elaborates on a method which could minimize current deficiencies without having severe impact on the huge amount of already existing evaluations and data. The method should have the capability to introduce stress-strain curves in future code editions.

Established in 1880, the American Society of Mechanical Engineers (ASME) is a professional not-for-profit organization with more than 127,000 members promoting the art, science and practice of mechanical and multidisciplinary engineering and allied sciences. ASME develops codes and standards that enhance public safety, and provides lifelong learning and technical exchange opportunities benefiting the engineering and technology community. Visit www.asme.org for more information.

The ASME Standards Technology, LLC (ASME ST-LLC) is a not-for-profit Limited Liability Company, with ASME as the sole member, formed in 2004 to carry out work related to newly commercialized technology. The ASME ST-LLC mission includes meeting the needs of industry and government by providing new standards-related products and services, which advance the application of emerging and newly commercialized science and technology and providing the research and technology development needed to establish and maintain the technical relevance of codes and standards. Visit www.stllc.asme.org for more information.

EXECUTIVE SUMMARY

For the determination of monotonic stress-strain curves, different approaches currently exist in the ASME code. Section VIII/2 and FFS-1 use predominantly a two power law approach based on Y-1 and U-table values for direct prediction of true stress-strain curves (in the following referred to as MPC approach). Sometimes, also a single power law approach for direct determination of true stress strain curves is used (RO). Section III uses a rational polynomial for determination of isochronous stress strain curves. It was a major aim of the current report to evaluate capabilities and limitations of the different methods using experimental results from literature and to elaborate on a method which could minimize current deficiencies without having severe impact on the huge amount of already existing evaluations and data. The method should have the capability to introduce stress-strain curves in future code editions. With respect to the different methods the results are the following.

The MPC-approach gives good results for low strains and for high strains. However, it shows a kink which is a result of switching between the two different power laws employed. Another problem concerns the determination of the ultimate tensile strain which will be discussed later.

The RO-approach as used in FFS-1 is a one power law approximation of the true stress-strain curve. In this respect it differs from the original Ramberg-Osgood (RO) method which is based on the engineering stress-strain curve and not on the true stress-strain curve. The ASME RO-approach leads to smooth looking curves but they often do not match the experimental values which is a result of the mathematical structure of the power law when engineering stress and strain is replaced by true stress and strain.

The rational polynomial can only be applied for small strains (up to 2%) but there are some difficulties to match with the high strain regime (particularly with ultimate tensile strain).

Best results were obtained with the original Ramberg-Osgood parameterization based on engineering stresses and strains (called in the following RO-eng).

$$e = \frac{s}{E} + K \left(\frac{s}{s_0} \right)^n$$

Where e is engineering strain, s is engineering stress, E is Young's modulus, s₀ is normalizing stress (usually 0.2% yield stress).

The constants K and n can be determined from yield stress and ultimate tensile stress under the assumption that both stress values belong to the stress-strain curve. Yield stress and 1.1 x ultimate tensile stress can be found in Sect. II /D stress tables (Tables Y-1 and U) which means that the engineering stress-strain curve is fully determined with already existing code data. The true stress-strain curve is obtained by plotting the true stress vs. true strain values. Comparison of this RO-eng method with experimental data revealed that this approach nicely agrees with experimental results and it also matches the MPC-values for low and high strains without showing a kink. Compared with the RO-method based directly on true stresses and strains, it leads to much better results because it does not have the numerical problems with fitting stress-strain data dependent on each other with one power law. Comparisons with the rational polynomial led to a fair agreement as discussed in appendix B.

The problem of determination of the ultimate tensile strain remains the same for all approaches based on ultimate tensile stress. The MPC-method proposes materials dependent values which are governed by the ratio between yield stress and ultimate tensile stress which may not always provide satisfactory solutions. An alternative which was used in this report is materials independently based on the difference between ultimate tensile stress and yield stress. Although more accurate values than the MPC-method could be obtained, the determination of ultimate tensile strains cannot be considered to

be fully satisfactory and further improvements should be envisaged. However, it could be shown that most accurate parameterizations can be obtained with measured ultimate tensile strains which demonstrate the capability of the RO-eng approach. All methods described work only for materials possessing stress-strain curves with a power law shape. This is the case for a vast majority of metals and alloys. Specific effects like Lueders strains cannot be built into the MPC-method but they could be successfully implemented into the RO-eng approach.

Based on all these results the RO-eng approach is proposed for implementation of monotonic stress-strain curves into the code. Usually, reference to Y-1 and U-Tables would be sufficient. Specific issues like Lueder's strain, ultimate tensile strain, expected deviations from power law, etc. could be introduced as notes into code tables.

The MPC-curves for tangent moduli show expectedly also a discontinuity at the transition from low strain to high strain. The RO-eng curve allows an analytic expression of the tangent modulus of true stress-strain curves without discontinuity.

Cyclic stress-strain curves fulfill usually a power law relationship but they are strongly dependent on material and even pre-treatment and they can therefore not be constructed from Y-1 and U-values. It is necessary to define them on a case to case basis. Existing cyclic stress-strain curves in Section VIII/2 seem to be based on published results. Although for cyclic stress-strain curves the differences between RO and RO-eng are almost negligible (because usually only low strains are considered) RO-eng is also recommended for establishing those curves. Data for additional cyclic stress-strain curves can be taken from the literature and databases (e.g. NIMS [25]), where much LCF-work has been published. The RO-eng approach enables simple reconstruction of cyclic stress strain curves even from LCF data as usually published. An important point concerns the consistency between monotonic stress-strain curves (determined from Y-1/U-tables) and cyclic stress-strain curves from other sources. It must be taken into consideration that cyclic softening and/or hardening happens relative to the monotonic data. To avoid misinterpretations, scaling may have to be performed when comparing data from different sources. For different sources, scaling with the ratio of yield stresses is proposed.

The cyclic stress-strain curves can be used for construction of the hysteresis loop by scaling with a factor of two.

Although quite consistent results could be established still a few points would need further research:

- Method of determination of ultimate tensile strain
- Clear criteria when Lueders stress and/or other irregularities must be considered
- Determination of amount of Lueder's stress to be included
- Further proof of RO-eng-concept with additional experimental data and link with Y-1/U-table values
- Establishing missing cyclic stress-strain curves from literature
- Activating of stress-strain data available in different laboratories of ASME members
- Coupling of establishment of stress-strain curves with ASME database activities.

1 INTRODUCTION

This project resulted from ASME Pressure Technology Codes and Standards (PTCS) Standards Committee requests to identify, prioritize and address technology gaps in PTCS Codes, Standards and Guidelines, and is intended to establish and maintain the technical relevance of ASME codes and standards products. In this context the inclusion of sound stress-strain curves for design purpose is required. As a first step a study shall provide:

- a. Literature review to evaluate material strength models and the required material parameters for high priority materials in Section VIII, Divisions 1, 2 and 3.
- b. Modification of existing, or development of new, models for the monotonic and cyclic stress-strain curves.
- c. Collection of the required material parameters for these models and introduction into Divisions 2 and 3.
- d. Preparation of a proposal for providing information on lower priority materials.
- e. Documentation of materials where data does not exist including a proposal for a test program.

After evaluation of the data and examination of potential constitutive models to be used, a recommendation will be made to ASME for an efficient and simplified format of conveying behavior for the purposes of design.

Special emphasis will be placed on the most common materials or high priority materials, as determined by ASME, used for construction such as

- Carbon steel (all strength levels)
- Chromium molybdenum (vanadium) steels like 1.25Cr-1Mo and 2.25 Cr-1Mo, including enhanced alloys (all strength levels)
- Ferritic –martensitic steels (e.g. 9-12% Cr) including enhanced alloys
- Stainless steels (austenitic, ferritic-martensitic, duplex, precipitation hardening)
- Nickel-base alloys (e.g. N06600, N06625 and N08800)
- Aluminum based alloys
- Titanium based alloys
- Copper based alloys
- Zirconium based alloys.

True stress-strain diagrams should be made available for inclusion into the code. Currently, different approaches for determination of stress-strain curves are in use: For the true stress strain curves Sect. VIII Div. 2 employs a two-slope approach discriminating between low plastic strains and high plastic strains. Cyclic stress-strain diagrams (which show basically the same behavior) are covered with a traditional Ramberg-Osgood parameterization and within Sect. III NH, another (different) method is used. In the case of Sect. III Div. 2, formulae to determine the true strain for a given true stress and the tangent modulus are given for certain classes of materials using Y-1 and U-table values. The current project should develop a procedure along the following guidelines.

- The procedure shall be able to predict true (and engineering) stress-strain curves for the classes of materials specified in the whole stress range from elastic to ultimate tensile stress.
- The curves shall be based on yield strengths and ultimate tensile strengths given in the Y-1 and U-tables.
- The procedure shall allow a quick determination of the whole true and engineering stress-strain curves in the range specified.
- The procedure should cover several Code needs (true stress-strain, engineering stress strain, cyclic stress strain) for a wide temperature range.

2 METHODS OF PARAMETERIZATION OF STRESS-STRAIN CURVES

2.1 Engineering Stress-Strain Curves

Attempts to predict stress strain curves properly are very old. Ramberg and Osgood reported on attempts to describe the plastic strain with a power law in 1943 [1].

$$e = \frac{s}{E} + K \left(\frac{s}{s_0} \right)^n \quad (1)$$

Where e is engineering strain, s is engineering stress, E is Young's modulus, s_0 is normalizing stress (usually the yield stress), K and n are fitting constants.

The designations e and s for engineering stress and engineering strain were chosen in agreement with the bulk of literature to differentiate between engineering stress-strain and true stress-strain. For the applications which will be discussed in this report describing the stress-strain behavior only until ultimate tensile stress and not further into the real necking regime, the well-known relations between engineering and true stress-strain (σ , ϵ) can be used:

$$\sigma = s(1+e) \text{ and } \epsilon = \ln(1+e) \quad (2)$$

For the true stress-strain curve often the term "flow curve" is used.

Equation (1) essentially states that the stress-strain curve of many metals and alloys in the region of uniform plastic deformation can be expressed by the simple power curve relation

$$\sigma = K e_p^n \quad (3)$$

Where e_p is the plastic strain, n is the strain-hardening exponent and K is the strength coefficient. Using the elastic strain e_{el} the relation

$$e = e_{el} + e_{pl} \quad (4)$$

becomes equivalent to the Ramberg-Osgood equation (1).

Although from the engineering stress-strain curve it is always possible (below necking) to calculate the true stress strain curve via relations (2) it is difficult to calculate for a given true stress σ the related true strain, ϵ , directly (without using the engineering data). Figure 1 shows an engineering stress-strain curve and a flow curve of 316 steel measured at room temperature [2]. The appearance of the engineering stress-strain curve is quite different to the true stress-strain curve which shows for the higher strains almost a linear shape. The difference becomes more visible in a logarithmic plot of the stresses as a result of the respective plastic strains as shown in Figure 2 and 3.

Before further discussing possible parameterizations of the true stress-strain curve I would like to elaborate on the engineering stress-strain curve and possibilities to predict its shape from s_{YS} , s_{UT} and E . The assumption that the yield stress is part of the curve given in equation (1) leads to the following:

$$e_{0.2} = \frac{\sigma_{0.2}}{E} + K \quad (5)$$

with $e_{0.2} = \frac{\sigma_{0.2}}{E} + 0.002$ one obtains for K the value of 0.002.

Assuming the ultimate tensile stress being part of the same curve one calculates:

$$e_{UTS} = \frac{s_{UTS}}{E} + 0.002 \left(\frac{s_{UTS}}{s_{YS}} \right)^n \quad (6)$$

or

$$\left(e_{UTS} - \frac{s_{UTS}}{E} \right) / 0.002 = \left(\frac{s_{UTS}}{s_{YS}} \right)^n \quad (7)$$

which finally leads to:

$$\log \left(\left(e_{UTS} - \frac{s_{UTS}}{E} \right) / 0.002 \right) / \log(s_{UTS} / s_{YS}) = n \quad (8)$$

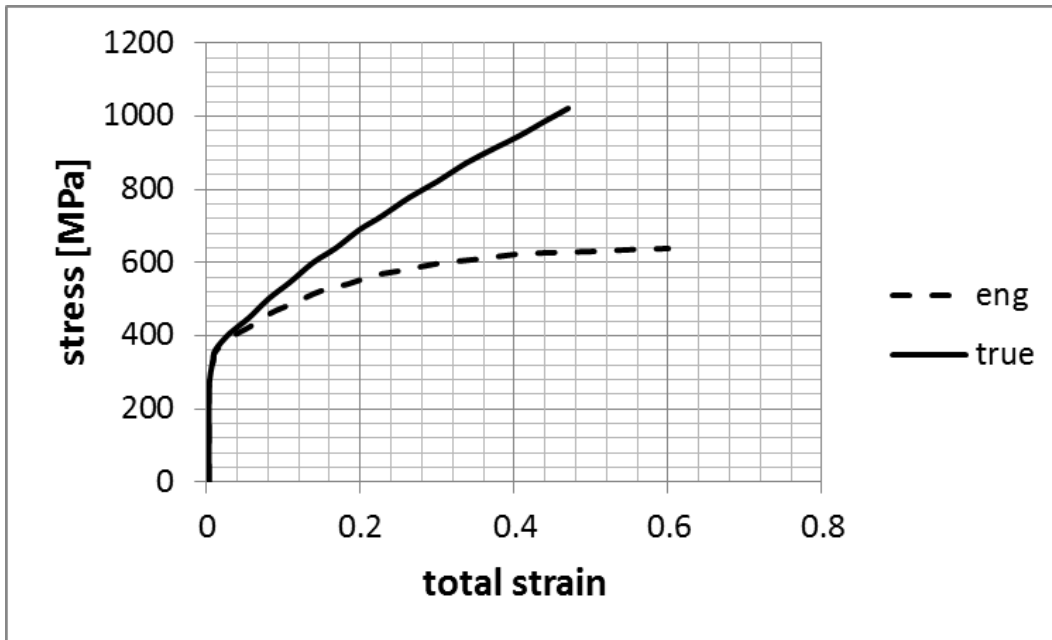


Figure 1—Engineering and True Stress-strain Curves for 316 Measured at Room Temperature

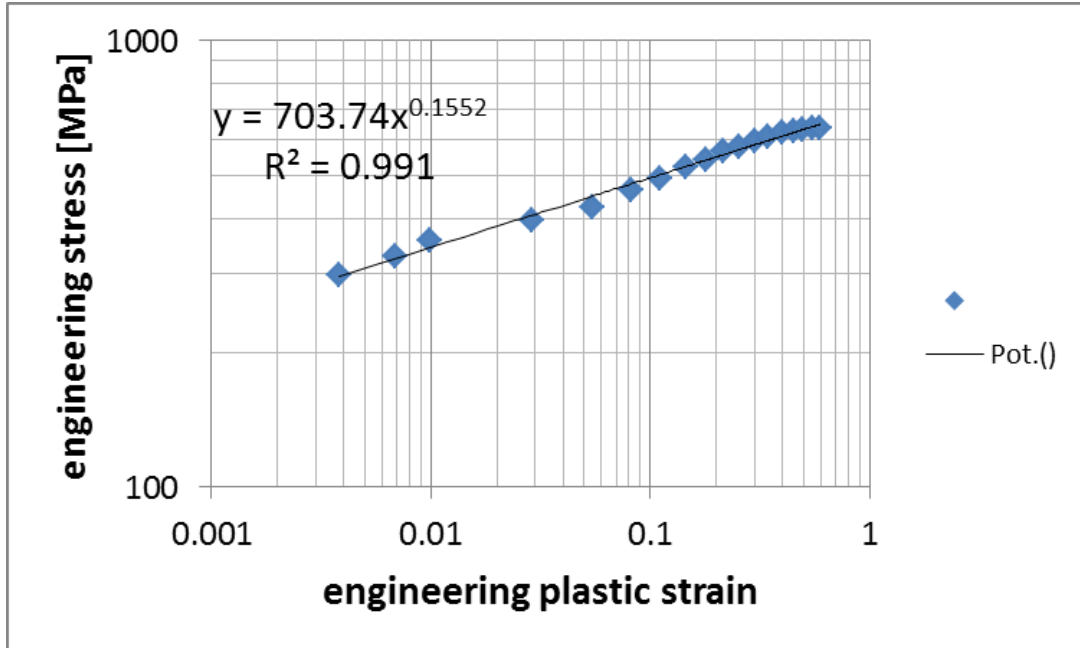


Figure 2—Engineering Stress vs. Engineering Plastic Strain for 316 Measured at Room Temperature

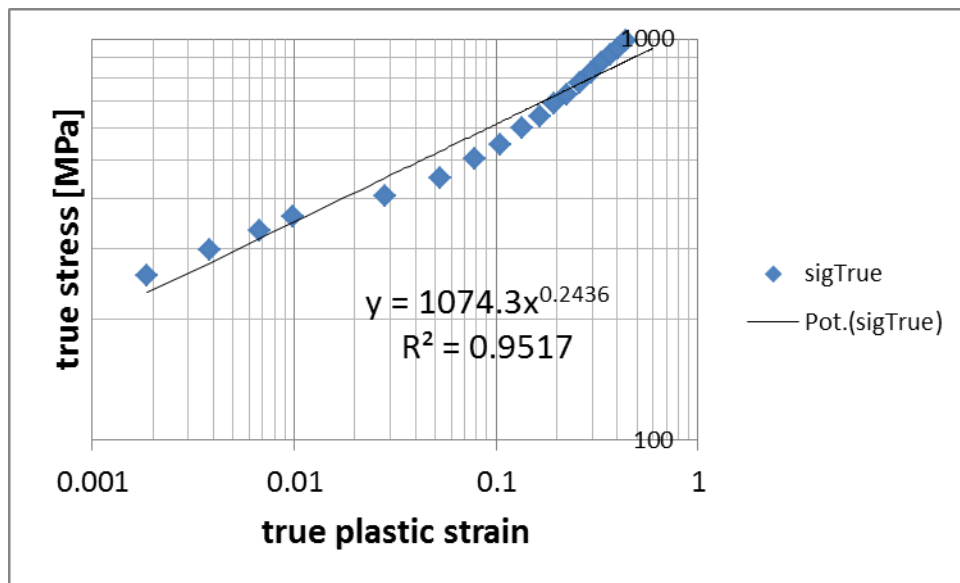


Figure 3—True Stress vs. True Plastic Strain for 316 Measured at Room Temperature

This means that under the given assumptions the stress-strain curve can be fully determined. One point which still remains open is the determination of e_{uts} . This will be discussed in a later section.

Within ASME also another model for establishing engineering stress-strain curves (particularly for low plastic strains) is employed. Discussions with Bob Swindeman concerning stress-strain curves for isochronous curves in ASME III Div. 5 triggered some discussions on the rational polynomial method which shall be introduced with Swindeman’s statement:

Yes, the basic equation is a rational polynomial. The equation may be written;

$$S = S_0 + [h (S_u - S_0) (ep)^{0.5}] / [1 + h (ep)^{0.5}]$$

This equation has the characteristic of a proportional limit: S_0 when ep is zero and an upper limit of S_u when ep is very large. (When $h (ep)^{0.5}$ is large compared to 1 the term cancels with the term in the numerator and one is left with $S_0 + S_u - S_0$ or S_u , the ultimate strength. The hardening parameter, h , may be calculated by inserting S_y for S and 0.2% for strain into the equation and solving for h .

$$\text{One gets } h = (S_0 - S_y) / [(S_y - S_u)(0.2)^{0.5}]$$

In our work on alloy 800H we noticed that S_0 was approximately $0.72S_y$.

The equation only works for engineering strains to a few percent but that is all that is needed for the isochronous curves and buckling analyses in III-NH. Other austenitic alloys may have different values for the ratio of proportional limit to 0.2% yield strength. The attractive feature of the simple approach is that one only needs the $Y-1$ value and the U value given in II-D. We recently used this equation for alloy 253 with some success. A more elaborate model using the rational polynomial was published by Joe Hammond and Vinod Sikka in 1977. See J. P. Hammond and V. K. Sikka, "Predicted Strains in Austenitic Stainless Steels at Stresses above Yield," pp. 309-322 in *Effects of Melting and Processing Variables on the Mechanical Properties of Steel*, MPC-6, ASME, New York, 1977.

This approach gives certainly very good values for austenitic materials but they were not more accurate than the procedure described above using Y_S and U_{TS} . A general application of this method needed determination of S_0 -values for other classes of materials which could be done but it needed an additional effort and further parameterization work. More information can be found in the literature [6][7]. A critical comparison of the results gained with the rational polynomial and with the Ramberg-Osgood fit for IN 800 H is given in Appendix II.

2.2 True Stress-Strain Curves

Many attempts were made to get a relation similar to equation (1) for the true stress-strain curves. Hollomon [3] proposed an approach similar to equation (3) also for the true stress strain curve.

$$\sigma = K \varepsilon_p^n \quad (9)$$

Cofie et al. made a similar attempt to get a one-power law fit of true stress-strain data specifically tuned to ASME needs [8] and they proposed a power law of the form

$$\frac{\varepsilon}{\varepsilon_0} = \frac{\sigma}{\sigma_0} + a \left(\frac{\sigma}{\sigma_0} \right)^n \quad (10)$$

for the true stress-strain curve particularly with respect to austenitic materials. The idea of this approach was the demand that the yield strength as well as the ultimate tensile strength must be points of the curve. This allowed the determination of a and n in equation (10) and consequently an analytical expression for the true stress-strain curve. The results of this approach were compared with others and a very good agreement amongst them was found. However, the agreement with real measurements turned out to be less convincing which can already be expected from the results shown in Figure 3.

The results shown in Figure 3 clearly demonstrate that a simple power-law type of fit cannot lead proper results, because there is no simple power law relationship between the true plastic strain and the true plastic stress. This is to some extent due to the structure of the relationship itself as quickly demonstrated in the following.

Let us assume for the engineering stress strain curve the validity of the following equation:

$$e = \left(\frac{s}{E}\right) + 0.002 \left(\frac{s}{s_{0.2}}\right)^n \quad (11)$$

Where s is engineering stress, e is engineering strain and E is Young's modulus.

In case of a true stress-strain curve the power law expression would become something like

$$\left(\frac{s(e+1)}{s_{0.2}}\right)^n \quad (12)$$

As $s_{0.2}$ is only for norming purpose it has not been converted further. Equation (2) can be written as:

$$\left(\frac{s}{s_{0.2}}\right)^n (e+1)^n \quad (13)$$

The second term is a polynomial with rational exponent which can be developed into a series which gives (taking only the first order term):

$$(1 + ne) \quad (14)$$

In other words the conversion from engineering to true stress adds an additional element to the power law describing the engineering curve which can be seen also from Figure 3. It is important to notice that a single power law fit to true stress-strain data is still used in current code documents as a possible alternative to the MPC 2-power law description. As long as this remains confined to small stresses only (e.g. cyclic stress-strain curves) this might be valid, but for the whole strain range (up to UTS) highly non-conservative assessments can be obtained.

This discrepancy between parameterization of engineering vs. true stress-strain curve is not at all new and it has been several times discussed in the literature. Equations like the Ludewik equation (12)

$$\sigma = \sigma_0 + K\varepsilon^n \quad (15)$$

or the similar Swift equation (13)

$$\sigma = K(\varepsilon_0 + \varepsilon)^{n'} \quad (16)$$

were proposed and deeper analysis of them can be found in the literature e.g. [2][4][5][9][10][11].

A general representation of a true stress-strain curve would be a multiple power law expression. Usually, two power law terms as shown in equation (17) are sufficient.

$$\varepsilon = \frac{\sigma}{E} + A\left(\frac{\sigma}{\sigma_0}\right)^n + B\left(\frac{\sigma}{\sigma_0}\right)^m \quad (17)$$

Such an approach is currently used for the determination of the true stress-strain curves in several ASME (e.g. Sect VIII /2) procedures. It allows a construction of true stress-strain curves from yield stress and ultimate tensile stress both given in tables Y-1 and U (MPC-method).

Due to its importance in current code procedures the method shall be described and analyzed in more depth.

The general expression is given as

$$\varepsilon_t = \frac{\sigma_t}{E_y} + \gamma_1 + \gamma_2 \quad (18)$$

With the two power law expressions

$$\varepsilon_1 = \left(\frac{\sigma_t}{A_1} \right)^{\frac{1}{m_1}} \quad \text{and} \quad \varepsilon_2 = \left(\frac{\sigma_t}{A_2} \right)^{\frac{1}{m_2}} \quad (19)$$

for the low stress portion and for the high stress portion. The exponent $1/m_2$ and the coefficient A_2 are mainly determined by the demand that the point $(\sigma_{UTS}, \varepsilon_{UTS})$ must be part of the curve. The expression m_2 is therefore an expression for the true ultimate tensile strain which is obviously based on earlier experimental findings. This is a critical point also for the determination of the engineering stress-strain curves (mentioned already above) which will be discussed separately later.

For the low stress portion ε_1 is demanded that the yield stress (more precisely the 0.2% proof stress) and the point when significant plasticity happens (ε_p) are points of the curve. The discrimination between low and high strain portion (H) is based on the difference between the actual true strain and a function H which depends on yield stress and ultimate tensile stress shown in equation (20).

$$\gamma_1 = \frac{\varepsilon_1}{2} (1.0 - \tanh[H]) \quad \gamma_2 = \frac{\varepsilon_2}{2} (1.0 + \tanh[H]) \quad (20)$$

To gain better insight into what numerically happens during this procedure we analyzed the behavior for 304L at room temperature where a set of measured data exists [14]. A yield stress of 258 MPa and an ultimate tensile stress of 617 MPa were assumed for the calculations. Additionally, Young's modulus of 196,000 GPa was used. The results can be seen from Figures 4 and 5. Gamma 1 and gamma 2 are the low stress related strain and the high stress related strain, respectively. The functions $(1.0 \pm \tanh[H])$ describe a smoothed step function between the two strains (Figure 4). The situation becomes better visible in Figure 5 where different results were plotted. It can be seen that the two strains ε_{p1} and ε_{p2} are really two different power functions which meet far above the calculated stress when ε_{p1} changes to ε_{p2} . It is obvious that a discontinuity occurs when changing from ε_{p1} to ε_{p2} control as reflected in the curve called MPC_value.

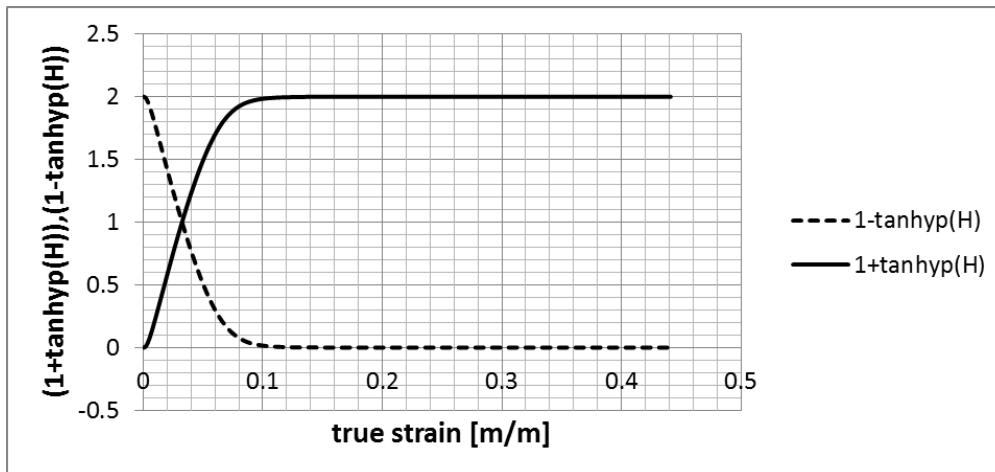


Figure 4—Shape of $(1+\tanhyp(H))$ and $(1-\tanhyp(H))$ for 304 L Stainless Steel at Room Temperature

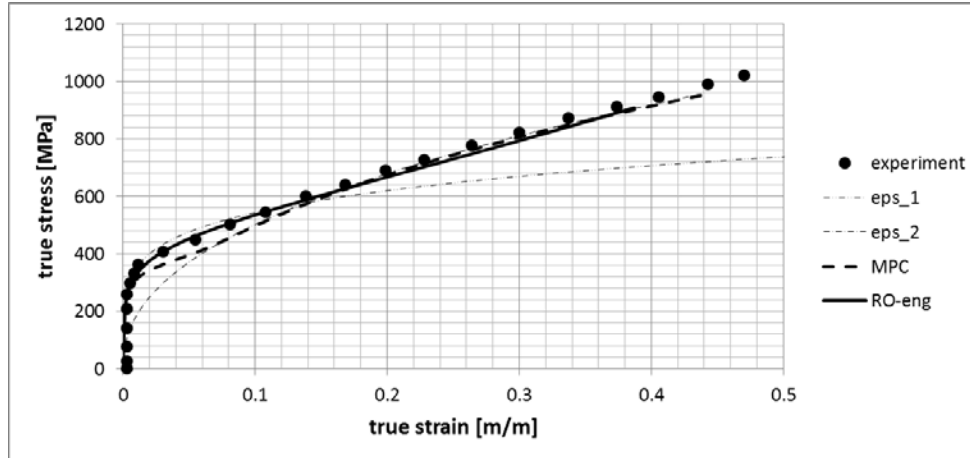


Figure 5—Comparison of Different Parameterizations of a True Stress-strain Curve for an Austenitic Steel at Room Temperature

Eps_1 and eps_2 are the two power law functions of the MPC approach. MPC represents the final results of the MPC procedure. RO-eng represents a Ramberg-Osgood fit performed in the engineering stress-strain frame from which the true stress-strain data were obtained and experiment means experimental data.

The real interesting comparison is the one with experimental data (experiment) which shows that in this case the agreement between MPC-values and experiment is good up to about 350 MPa (eps_1) and for stresses above 600 MPa (eps_2). But between 350 and 600 MPa the agreement is not good at all. However, a really good prediction of the experimental data is found with the RO-eng approach which was based on the engineering stress-strain curve from which the true stress-strain values were determined according to equations (2).

Similar analyses of experimental data from for different materials led to the same result. The MPC-procedure could well describe the low strain and the high strain regime, but there was always a portion of the stress-strain curve where at the change from low to high strain a discontinuity occurred. It became also evident that the RO-eng curve determined for the engineering stress-strain curve and converted into a true stress-strain curve gave the best agreement with the experimental data.

In the following improvements of the MPC-procedure to smoothen the difference between the low strain and the high strain portion will be discussed.

One problem is the definition of the function H which is exclusively responsible for the switch. Using the notation of ASME VIII/2 with σ_t , true stress, σ_{ys} , engineering yield stress and σ_{uts} , engineering ultimate tensile stress, H is defined as:

$$H = \frac{2 \left[\sigma_t - \left(\sigma_{ys} + K \left\{ \sigma_{uts} - \sigma_{ys} \right\} \right) \right]}{K \left(\sigma_{uts} - \sigma_{ys} \right)} \quad (21)$$

As K is also defined as a polynomial in σ_{ys}/σ_{uts} the whole expression depends only on the difference between σ_t and a constant (for given σ_{ys} and σ_{uts}). This term does not provide any possibility for modifications.

As smoothening approach it was tried to determine the point where the slopes of the low strain and the high strain curves are the same:

Let us start from the assumption that we have two power laws describing different portions of one curve:

$$\varepsilon_1 = \left(\frac{1}{A_1}\right)^{\frac{1}{m_1}} \sigma_T^{\frac{1}{m_1}} \quad \text{and} \quad \varepsilon_2 = \left(\frac{1}{A_2}\right)^{\frac{1}{m_2}} \sigma_T^{\frac{1}{m_2}} \quad (22)$$

The stress where the slopes of both curves are the same, σ_T^{equ} , can be determined by setting the derivatives of the two curves to equal which leads to:

$$\sigma_T^{\text{equ}} = \frac{\left(\frac{1}{A_2}\right)^{\frac{1}{m_2}} \frac{1}{m_2}}{\left(\frac{1}{A_1}\right)^{\frac{1}{m_1}} \frac{1}{m_1}} \quad (23)$$

In a next step the curve describing the higher stress portion is shifted by the difference between the strains at σ_T^{equ} towards lower strain. The resulting curve is shown in Figure 6 as “equal slope.” The other curves shown are the same as the ones shown already in Figure 4 and Figure 5. The agreement with the experimental data is now considerably better up to a strain of about 0.1. However, there is now a higher deviation from the measured data at higher strains.

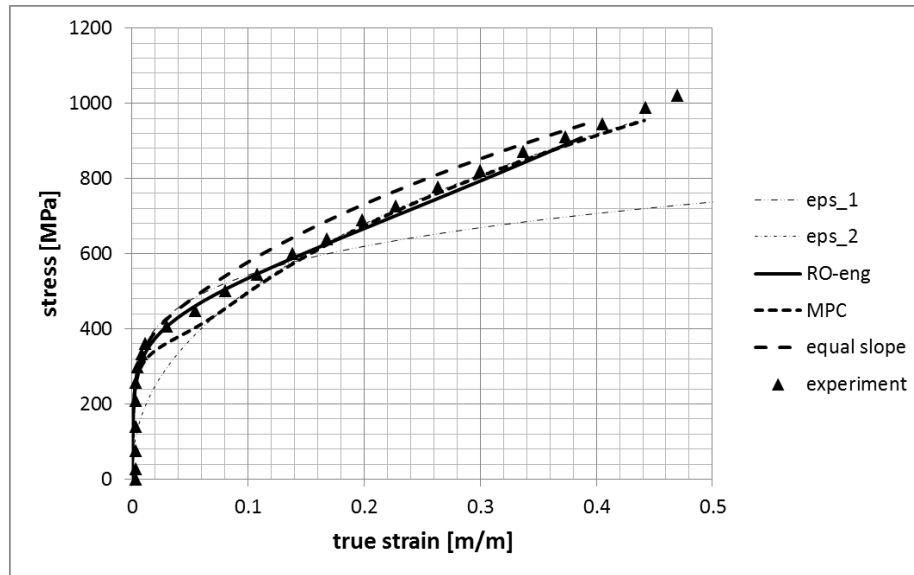


Figure 6—Comparison of a Modified MPC True Stress-strain Curve (Equal Slope) with the Other Stress-strain curve parameterizations shown in Figures 4 and 5

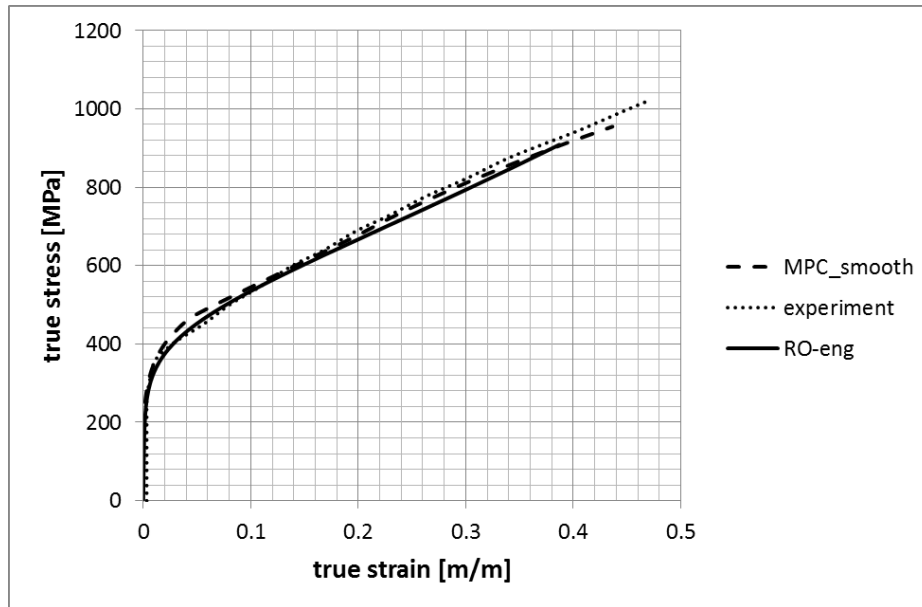


Figure 7—Comparison of Results from MPC and RO-eng Results Omitting Data-points at the Transition from Low Strain to High Strain for the MPC Approach

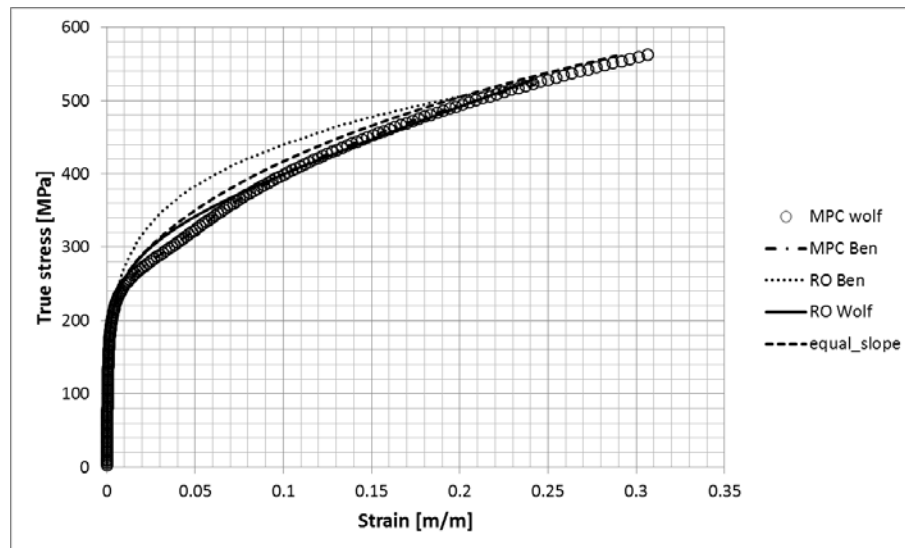


Figure 8—Comparison of Different True Stress-strain Parameterizations

In Figure 8, MPC Ben and RO Ben Refer to the ASME FFS-1 Procedure Provided in [15], MPC Wolf represents the own evaluation according to ASME VIII/2 which is the same as FFS-1. RO Wolf is the Ramberg-Osgood fit starting from the engineering stress-strain curve, equal slope stands again for the MPC-procedure modified by fitting low and high strain regimes at equal slopes of the two power laws.

The second smoothing procedure was just to omit the data in the cross-over regime and draw a smooth curve. The result is compared in Figure 7 with experimental data and the engineering stress-strain based Ramberg-Osgood curve. This leads to an extremely good agreement of all three curves. The only problem remains the smoothing procedure which is a bit of an arbitrary procedure.

Similar results were also obtained with 2.25 Cr-1Mo in a comparison with the ASME FFS-1 evaluation provided by Ben Hantz [15] which was summarized in Figure 8.

It becomes obvious that the MPC-Ben solution gives exactly the same results as MPC Wolf which means that the ASME FFS-1 MPC procedure fully agrees with the MPC-procedure adopted for this report. RO Wolf is the RO-parameterization based on the engineering stress-strain curve (usually called RO-eng) whereas RO Ben is a single power law fit of the true stress-strain curve similar to the Hollomon or Coffie-approach (see equ. 9 and 10). As highlighted in equations 11-13 a single power law fit is normally not able to map the true stress strain curve properly and it leads in almost all cases to an extended arc between YS and UTS, leading to exaggerated stresses.

3 THE DILEMMA OF FINDING THE (USUALLY NOT AVAILABLE) ULTIMATE TENSILE STRAIN

Before recommendations concerning applicability of the different methods will be given another critical issue must be highlighted; the determination of the ultimate tensile strain.

3.1 Rasmussen Procedure

The discussion will commence with the ideas of Rasmussen [16]. He analyzed the ultimate tensile strain for austenitic, ferritic and duplex steels and he obtained the best correlation with the parameterization (see also Figure 9):

$$\varepsilon_u = 1 - \frac{\sigma_{0.2}}{\sigma_u} \quad (24)$$

Where ε_u is ultimate engineering tensile strain, $\sigma_{0.2}$ is engineering proof stress, σ_u is engineering ultimate tensile stress.

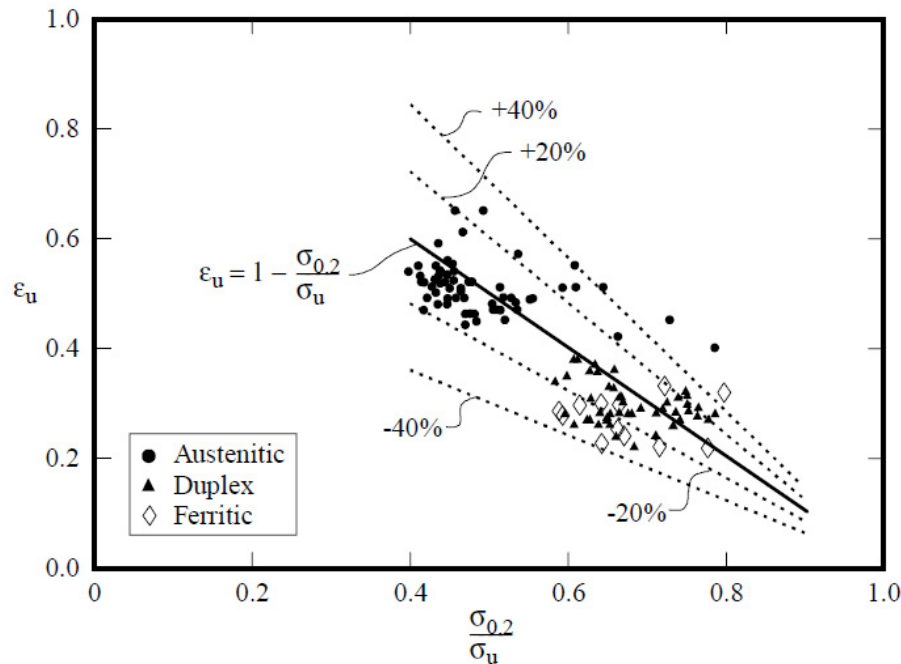


Figure 9—Correlation between Yield Stress, Ultimate Tensile Stress and Ultimate Tensile Strain (replotted from Rasmussen [16])

The high scatter of data is not surprising for experimentally determined mechanical values. However, my own trials with other experimental data from the literature did not show the behavior anticipated by Rasmussen. Also the ultimate tensile strains of ferritic and duplex materials in Figure 9 seem to be rather independent from $\sigma_{0.2}/\sigma_u$.

3.2 The MPC-approach

From relation (24), which is given in the MPC procedure, the true ultimate tensile stress can be obtained using

$$\sigma_{uts,t} = s_{uts} \exp(m_2) \quad (25)$$

with material dependent values given in Table 1. Using the usual conversion between true stress/strain and engineering stress strain (equ 1) one obtains with $\sigma_{\text{uts},t} = s_{\text{uts}}(1+e)$ for e_{uts} :

$$e_{\text{uts}} = \frac{\sigma_{\text{uts}}}{s_{\text{uts}}} - 1 \quad (26)$$

or

$$\exp(m_2) - 1 = e_{\text{uts}} \quad (27)$$

This means that under the assumption of the validity of Table 1 the strain values at ultimate tensile stress can be determined which allows the construction of engineering stress-strain curves only with yield stresses and ultimate tensile stresses given in Y-1 and U tables.

Table 1—Parameters for Ultimate Tensile Strain (m_2) and for Start of Plastic Deformation (ϵ_p) for Different Classes of Materials as Defined in the MPC ASME VIII/2 Procedure

Material	Temperature Limit	m_2	ϵ_p
Ferritic Steel	480°C (900°F)	$0.60(1.00 - R)$	2.0E-5
Stainless Steel and Nickel Base Alloys	480°C (900°F)	$0.75(1.00 - R)$	2.0E-5
Duplex Stainless Steel	480°C (900°F)	$0.70(0.95 - R)$	2.0E-5
Precipitation Hardenable Nickel Base	540°C (1000°F)	$1.90(0.93 - R)$	2.0E-5
Aluminum	120°C (250°F)	$0.52(0.98 - R)$	5.0E-6
Copper	65°C (150°F)	$0.50(1.00 - R)$	5.0E-6
Titanium and Zirconium	260°C (500°F)	$0.50(0.98 - R)$	2.0E-5

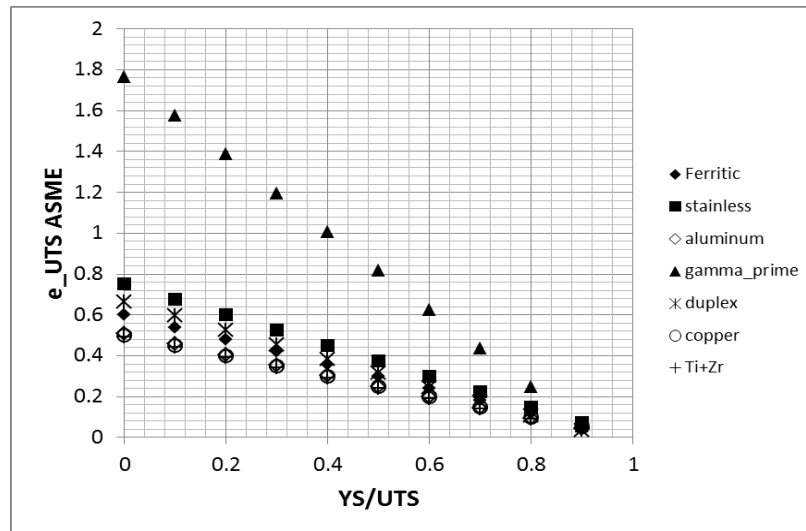


Figure 10—Ultimate Tensile Strains Determined According to Table 1 for Different Classes of Materials as Function of Ratio between Yield Stress and Ultimate Tensile Stress

MPC relations are straight lines when plotted against YS/UTS as shown in Figure 10. However, there is a differentiation between the different types of materials. For low values of YS/UTS the ultimate tensile strain for gamma prime hardening superalloys would exceed 100% which does not sound reasonable. As gamma prime hardening superalloys expectedly have a high YS/UTS ratio this

discrepancy is most probably not very significant. When YS and UTS are very close (i.e. YS/UTS close to 1) negative ultimate tensile strains are calculated which leads to erroneous results as shown later. Also, unfortunately, traditional materials like austenitic steels do not necessarily follow the expectations as shown in Figure 11. To improve the correlation another approach was attempted which will be described in the following.

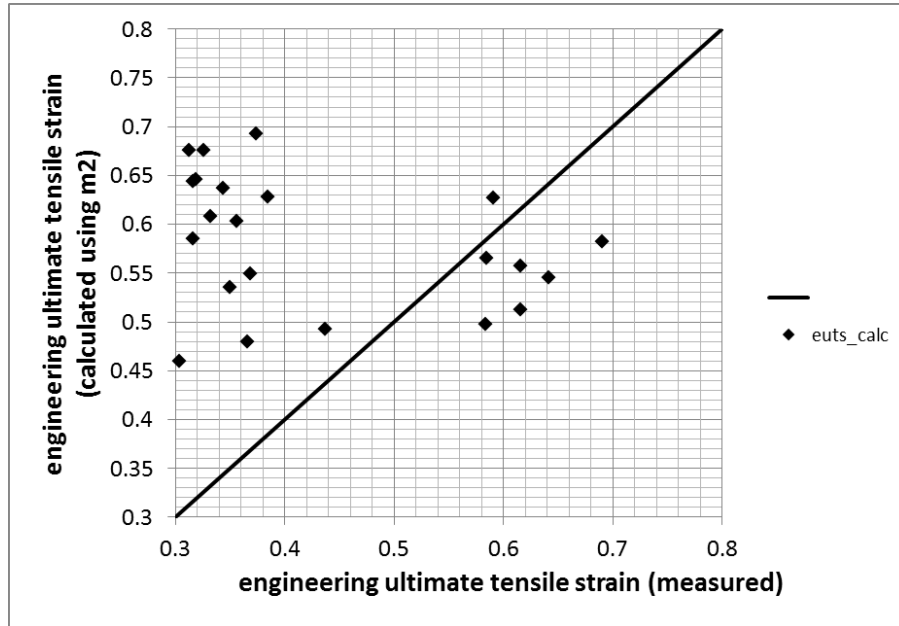


Figure 11—Comparison of Predicted and Measured Ultimate Tensile Strains Experimental Data Exclusively from [1]

3.3 The UTS-YS Approach

Let us start with equation (24) which can be re-written using the notation of equation (28):

$$\varepsilon_u = \frac{\sigma_u - \sigma_{0.2}}{\sigma_u} \quad (28)$$

The difference between the ultimate tensile stress and the yield stress determines in first order the slope of the inelastic part of the engineering stress-strain curve according to the relation

$$\frac{\sigma_u - \sigma_{0.2}}{\varepsilon_u - \varepsilon_{0.2}} \quad (29)$$

Assuming that 0.002 is small compared with the ultimate tensile strain we try to correlate the ultimate tensile strain with the difference between ultimate tensile stress and the yield stress.

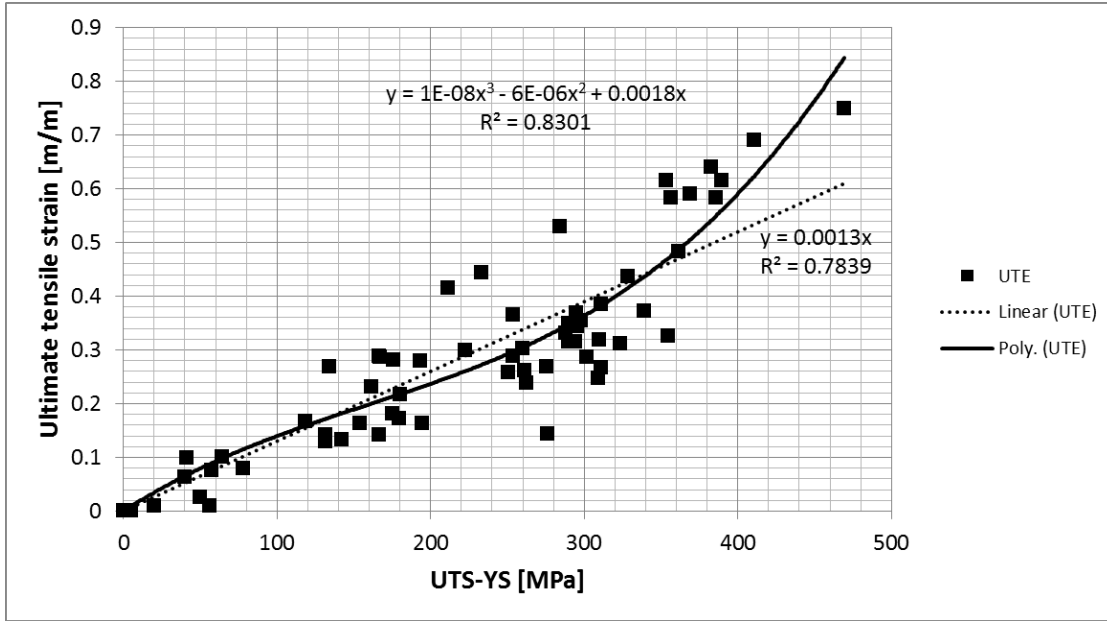


Figure 12—Experimentally Determined Ultimate Tensile Strains (see Table 1) as a Function of the Differences between Ultimate Tensile Stress and Yield Stress

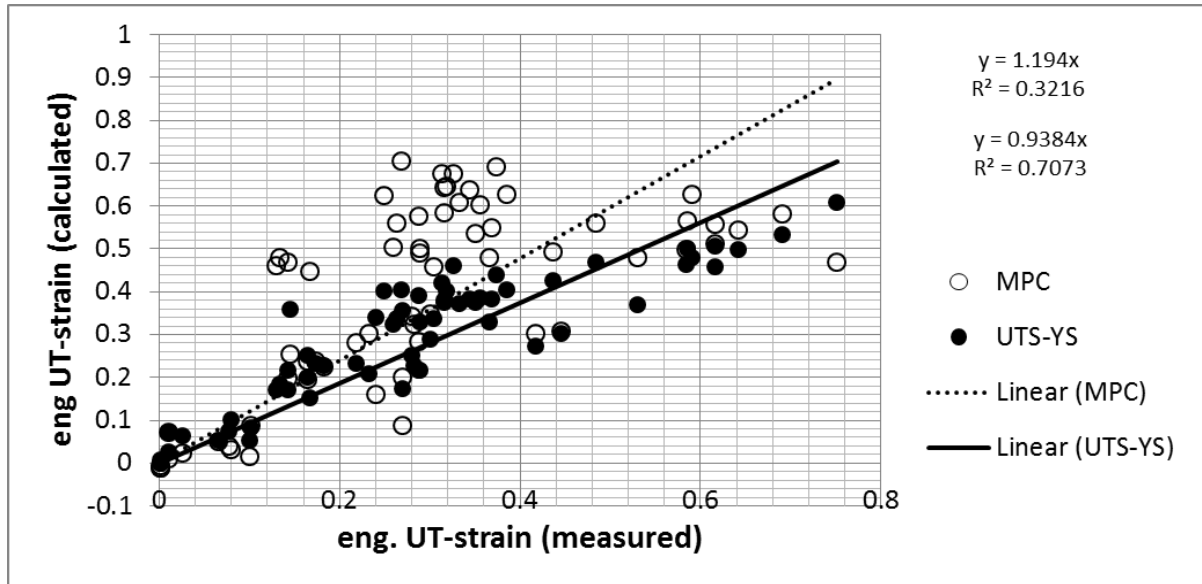


Figure 13—Comparison between Calculated and Measured Ultimate Tensile Strains

In Figure 13, MPC Refers to Strains Determined According to Table 1. UTS-YS Refers to the Third Order Polynomial Shown in Figure 12.

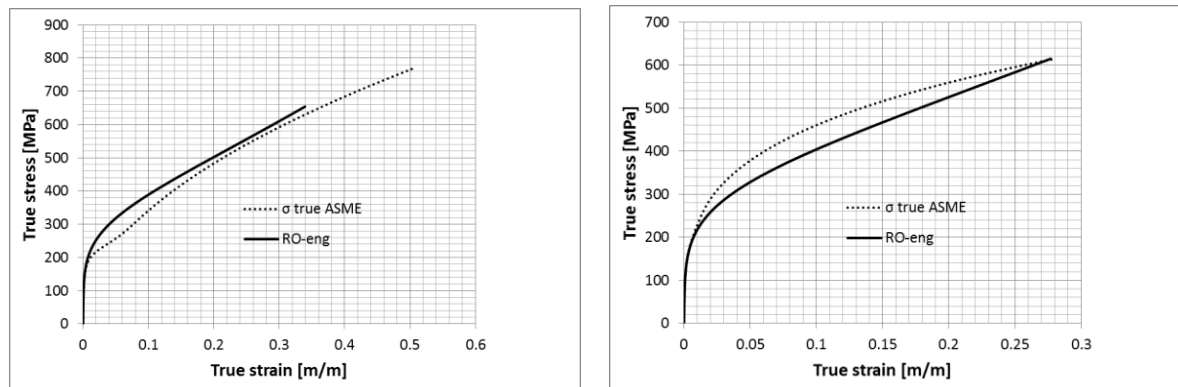
Table 2—Measured Ultimate Tensile and Yield Stresses

UTS	YS	UTE	UTS-YS	YS/UTS	material	m ₂
1222	630	0.1	592	0.51554828	steel	0.29067103
1220	1170	0.026	50	0.95901639	steel	0.02459016
1320	1300	0.01	20	0.98484848	steel	0.00909091
436	256	0.218	180	0.58715596	steel	0.24770642
518	343	0.183	175	0.66216216	steel	0.2027027
520	366	0.164	154	0.70384615	steel	0.17769231
853	796	0.077	57	0.93317702	steel	0.04009379
245	79	0.289	166	0.32244898	steel	0.40653061
733	264	0.751	469	0.36016371	aust	0.38390177
239	121	0.167	118	0.50627615	aust	0.37029289
259	128	0.13	131	0.49420849	aust	0.37934363
272	130	0.134	142	0.47794118	aust	0.39154412
255	124	0.142	131	0.48627451	aust	0.38529412
801	760	0.1	41	0.94881398	ti	0.01559301
944	866	0.08	78	0.91737288	ti	0.03131356
714	439	0.27	275	0.61484594	ti	0.18257703
837	837	0.002	0	1	ti	-0.01
706	572	0.27	134	0.8101983	ti	0.08490085
825	563	0.24	262	0.68242424	ti	0.14878788
935	935	0.002	0	1	ti	-0.01
851	846	0.002	5	0.99412456	ti	-0.00706228
660	277	0.642	383	0.4200627	aust	0.43495298
504	210	0.369	294	0.41586867	aust	0.4380985
466	157	0.319	310	0.33579882	aust	0.49815089
660	270	0.616	390	0.40961338	aust	0.44278997
478	168	0.385	311	0.35014409	aust	0.48739193
449	154	0.344	295	0.34254992	aust	0.49308756
662	305	0.584	356	0.46145833	aust	0.40390625
507	217	0.35	290	0.42857143	aust	0.42857143
478	224	0.289	254	0.46897547	aust	0.3982684
671	261	0.691	410	0.38848921	aust	0.45863309
483	144	0.374	339	0.29857143	aust	0.52607143
454	166	0.332	288	0.3662614	aust	0.47530395
652	419	0.445	233	0.64232804	aust	0.26825397
501	334	0.288	167	0.66712517	aust	0.24965612
470	294	0.282	176	0.62609971	aust	0.28042522
609	248	0.484	361	0.40656852	aust	0.44507361
459	298	0.232	161	0.64864865	aust	0.26351351
440	179	0.263	261	0.40752351	aust	0.44435737
568	199	0.591	369	0.35072816	aust	0.48695388
474	176	0.356	298	0.37117904	aust	0.47161572
443	150	0.316	294	0.33748056	aust	0.49688958
615	287	0.437	328	0.46636771	aust	0.40022422
516	256	0.304	260	0.4959893	aust	0.37800802
496	195	0.287	301	0.39305556	aust	0.45520833
645	260	0.585	385	0.40277778	aust	0.44791667
515	161	0.326	354	0.31191432	aust	0.51606426
472	182	0.316	290	0.38596491	aust	0.46052632
640	287	0.616	353	0.44827586	aust	0.4137931
485	232	0.366	254	0.47727273	aust	0.39204545
470	146	0.313	323	0.3113069	aust	0.51651982
599	388	0.417	211	0.64787112	aust	0.26409666
492	299	0.28	193	0.60784314	aust	0.29411765
459	209	0.259	250	0.45495495	aust	0.40878378
544	260	0.53	284	0.47782003	aust	0.39163498
478	169	0.249	309	0.35353535	aust	0.48484848
436	125	0.268	311	0.28751975	aust	0.53436019
374	152	0.3	222	0.40641711	al	0.2982631
348	308	0.065	40	0.88505747	al	0.04937011
476	420	0.01	56	0.88235294	steel	0.07058824
449	385	0.101	64	0.85746102	steel	0.08552339
551	385	0.142	166	0.69872958	steel	0.18076225
546	352	0.165	194	0.64468864	steel	0.21318681
504	325	0.173	179	0.64484127	steel	0.21309524
1457	1181	0.145	276	0.81056966	gamma prime	0.22691764

UTE refers to ultimate tensile strains according to Figure 12, whereas m_2 refers to the ultimate tensile strains determined according to the MPC procedure (Table 1).

Figure 12 shows the results of this correlation based on data coming from a variety of different materials as shown in Table 2. The correlation with UTS-YS is surprisingly good. Most simple parameterization can be made with a linear function or a bi-linear function. The best fit is obtained with a 3rd order polynomial. Several attempts to normalize UTS-YS by some stress (YS, UTS, E) made the correlation worse and therefore no further change was made (although a non-normalized stress does not look like a very physical solution). The real surprising result was the comparison with the MPC procedure for UT-strain determination which is shown in Figure 13. The MPC-data were calculated from m_2 as determined according to Table 1. The UTS-YS-data were determined with the 3rd order polynomial just described. Both calculated values were compared with the experimental results given in Table 2. Ideally a straight line with slope 1 is expected. It can be seen that the UTS-YS-approach leads to much better results than the MPC-procedure. It is fair to say that the scatter in experimental data coming even from one batch of material is high and therefore sometimes significant discrepancies between calculated and measured values cannot be avoided. Basically, this would not be an extremely severe problem if the m_2 -values as well as the ultimate tensile strain would not have an impact on the shapes of the MPC-curve and the RO-eng curve because they directly define the exponent in the power functions.

This shall be highlighted taking an austenitic steel as an example. The experimentally determined properties were YS: 156 MPa, UTS: 466 MPa, UT-strain: 0.319. Yield stress and UTS were used for the determination of the stress-strain curve according to MPC and RO-eng procedures. The results are shown in Figure 14a. The MPC-approach leads to high UT-strains and the previously discussed change from low strain to high strain regime is clearly visible. The RO-eng approach with the UTS-YS correlation for the ultimate tensile strain leads to a smooth curve and a quite good prediction of the ultimate tensile strain. Figure 14b shows the result when m_2 is set to meet the experimental UT-strain value and the RO-eng curve is also determined by the measured UT-strain. The RO-eng curve stays pretty much the same (which is no surprise because of the small difference between measured UT-strain and calculated one). However, the changes in the MPC-curve become significant. The curve smoothens out, and the stress values also change. The value at a strain of 0.1 increases by more than 25% from 340 MPa to 460 MPa.



(a) as calculated

(b) using measured UT-strain

Figure 14—Comparison of RO-eng and MPC Curves as Calculated (a) and Using the Actually Measured Ultimate Tensile Strain (b)

This is only one example demonstrating the necessity for a sound determination of the ultimate tensile strain. Since several parameterizations based on yield stress (Y-1) and ultimate tensile stress (U) need the ultimate tensile strain the determination of this quantity needs specific attention. It is obvious that the current MPC-procedure does not always lead to very accurate results. However, it is also not clear that the UTS-YS correlation covers really the variety of several classes of materials. It is therefore strongly recommended to perform further research into this important issue.

4 CRITICAL ASSESSMENT OF THE DIFFERENT APPROACHES USING ACTUAL STRESS-STRAIN CURVES

In the previous sections the capabilities and problems of different approaches for the determination of stress-strain curves from yield stress and ultimate tensile stress were discussed. Now the different classes of materials shall be highlighted in more detail. Generally it can be stated that (except the question of ultimate tensile strain) no problems are expected in all cases where the engineering stress-strain curve can be described by a power law relationship. Difficulties will emerge when deviations from the power law occur. It turned out that the temperature is only of minor importance concerning the parameterization of stress strain curves. However, strain-rate effects or differences in the materials response to tensile or compression are not included in the current approach. It is also important to stress that the considerations are limited to strains below where necking occurs. For higher strains ideally plastic deformation (without strain correction) should be used. This is not only valid for elevated and high temperatures; this is generally true for several types of strain rate dependence. From this point of view it seems to be justified to limit the construction of stress-strain curves to the same boundary assumptions as the ones valid for Y-1 and U-Tables. Stress-strain curves comparing results from the different methods with experimental data are shown in Appendix C.

4.1 Carbon Steels

Although these steels are frequently used and they were also very well investigated they provide some challenges for the determination of stress-strain curves as shown in Figure 15 [17]. It is well known that low carbon steels ($C < 0.25-0.30\%$) tend to form Lueders bands which lead to a constant stress portion of the curve. The mechanism that stimulates such behavior is known as "dynamic strain aging," or the pinning of dislocations by interstitial atoms (in steels, typically carbon and nitrogen), around which "atmospheres" or "zones" naturally congregate. These so-called Cottrell clouds hinder the dislocation movement until a certain "break-away" stress is reached. This behavior is often accompanied by an upper and lower yield stress. Neither the occurrence of this phenomenon nor the amount of constant strain can be predicted in a way that it could be used for our assessment. As rules of thumb it can be assumed that:

- It is common to low-carbon steels and certain Al-Mg alloys
- It remains usually limited to temperatures below about 150 C
- Typical constant strain ranges at yield are 0.02 [m/m]
- The difference between upper and lower yield point is negligible for our considerations
- It seem to vanish for pre-treated steels
- It only happens when the yield point is reached for the first time. It is therefore irrelevant for cyclic deformation.

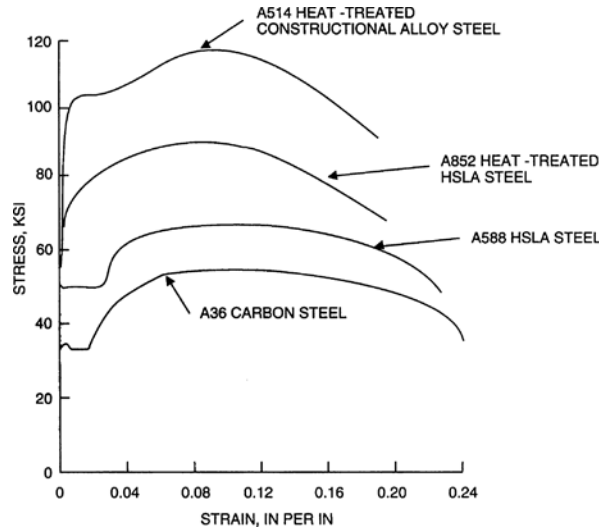


Figure 15—Stress-strain Curves of Different Carbon Steels [17]

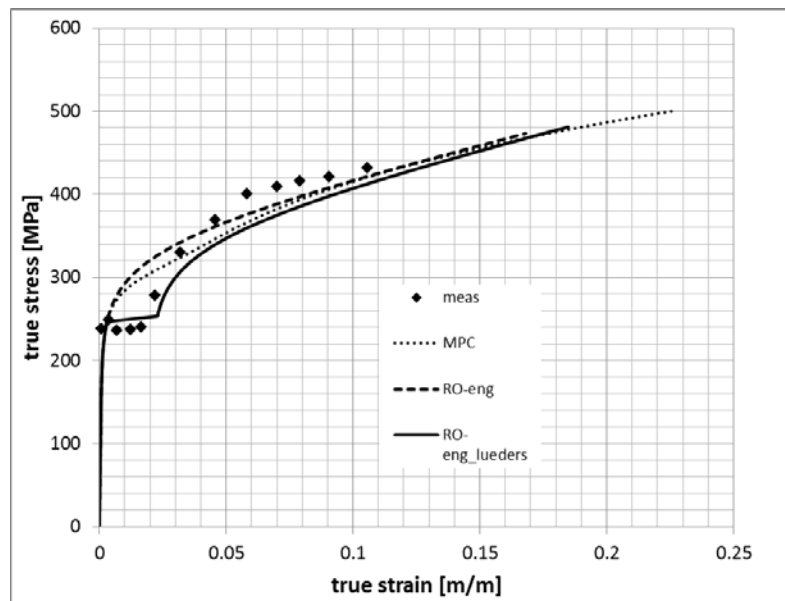


Figure 16—Stress-strain Curves for SA-36 Determined According to MPC and RO-eng Procedures without Lueders Strain Corrections

In Figure 16, RO-eng_lueders refers to the Lueders corrected RO-eng procedure.

In a good approximation the pronounced yield point can be taken as an equivalent to the proof stress. This is obviously also the case for Table Y-1 values where no discrimination between yield point and proof stress is made. Table Y-1 and U values were taken from ASME II-D to predict the A36 (SA-36) behavior shown in Figure 15. The results are shown in Figure 16. The “meas” points were taken from Figure 15 and the MPC and RO-eng curves were determined with the Table IID values for this steel. It can be seen that the agreement in the Lueders part of the stress-strain curve is not very good and it can also be seen that the kink calculated by the MPC-method is only a calculation effect which

has nothing to do with yield point behavior. Taking the “rules of thumb” mentioned above into consideration an attempt at modifying the RO-eng procedure was made in the following way:

- calculate the curve without modification
- consider the proof stress as yield point
- shift the strains above the yield point by 0.02.

The results are shown as RO-eng_lueders in Figure 16 and a good agreement with A36 shown in Figure 15 is found.

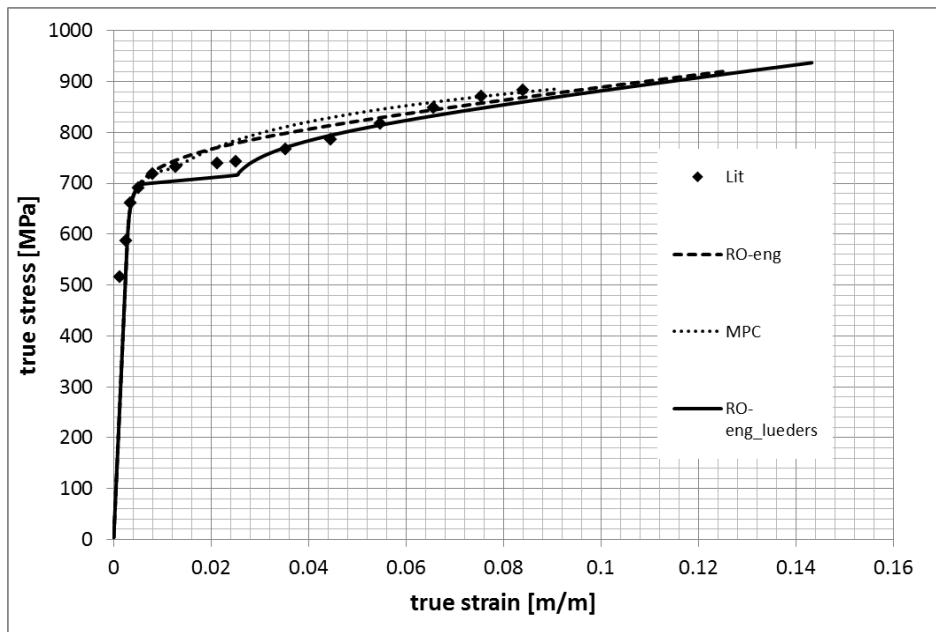


Figure 17—Comparison of Results from MPC and RO-eng Parameterizations of A514 (see Figure 15) with the Result from the Lueders-modified RO Approach (RO-eng_lueders)

The same procedure could also parameterize the A514 curve as shown in Figure 17. In this case yield stress and ultimate tensile stress were determined from the curve directly as for this material no Y-1 and U-values exist. It looks like this simple rule would have the capability to handle Lueders-strains but this must be further explored.

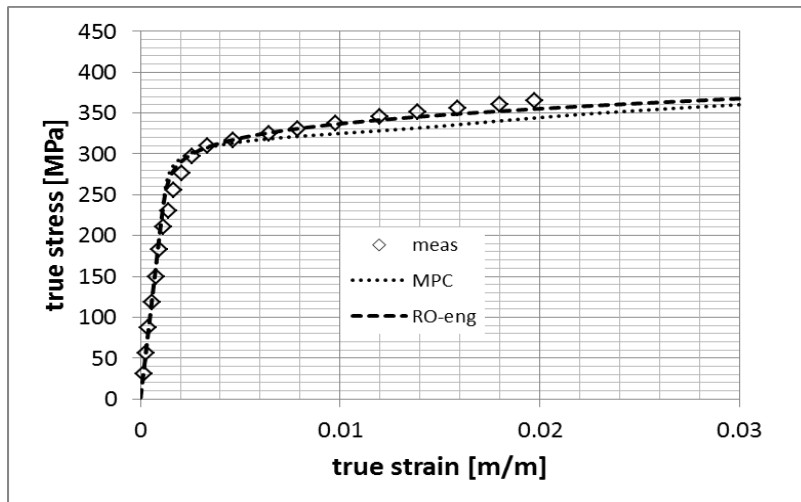


Figure 18—Stress-strain Curve of a Carbon Steel Without Occurrence of Lueders Strain

Figure 18 demonstrates how the RO-eng approach gives more accurate results concerning the shape of the curve. However, the ultimate tensile strains are not correctly reproduced.

In case no pronounced yielding is observed the experimental values can be well reproduced by RO-eng and MPC procedures (except ultimate tensile strain) as shown in Figure 18.

In conclusion, it can be stated that the phenomenon of yield points for carbon steels is difficult to generalize because it happens for several strength levels (including HSLA and TMT). Current Y-1 tables also do not discriminate between yield point and proof stress. The current MPC-procedure does not take this phenomenon explicitly into consideration. The RO-eng approach could be modified to account for yield point phenomena. Taking materials scatter and other uncertainties into consideration the question remains if for assessments like J-Integral or strain energy it would not be sufficient to work with a power law type of approach neglecting yield point phenomena.

4.2 Ferritic Steels

Engineering stress-strain curves for this class of materials follow usually a power law. Few exceptions from this rule are reported and it might be that for low alloy steels and low carbon contents yield point phenomena occur. This can be even the case for one type of material like 2.25 Cr- 1Mo in normalized/tempered condition. Whereas in [18] a yield point was observed at room temperature, no such phenomenon was found in [19]. The differences were mentioned, but not further commented. The power law shape of the stress-strain-curves remains for several temperatures (see appendix C). The other points concerning the MPC-procedure and the RO-eng procedure remain as previously discussed.

4.3 Martensitic Steels

Similar to ferritic steels also the martensitic steels follow usually a power law and can therefore be well described by a RO-eng and MPC approach.

4.4 Austenitic Steels

The stress-strain curves of austenitic steels usually follow also a power law. Sometimes a two-slope behavior is found as demonstrated in Figure 19 with an example.

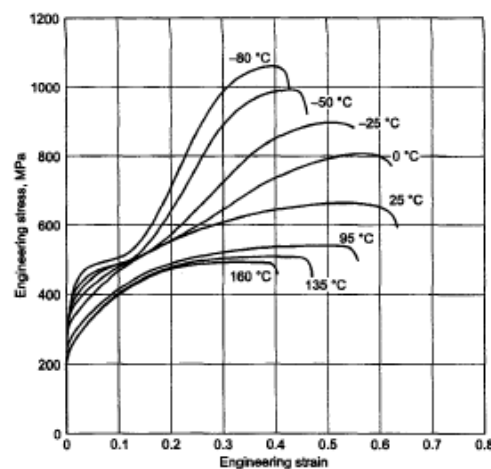


Figure 19—Occurrence of Secondary Hardening for Austenitic Steel at Temperatures below Room Temperature [18]

This behavior varies by alloy stability, with alloys like 201 and 301 showing pronounced two-slope behavior above room temperature, while stable alloys like 316 and 310 showing it only at sub-zero temperatures [26].

For inclusion of such effects even the engineering stress-strain approach would need a two-power law parameterization. For cases where the two slope shape occurs below room temperature it is fair to say that the room temperature curve provides at least a conservative assessment and it should be clarified if these effects need to be considered in future code editions.

4.5 Gamma Prime Hardening Superalloys

Most difficulties for this class of materials come from sometimes occurring large differences in the expected ultimate tensile strains which shall be highlighted taking IN-718 as an example.

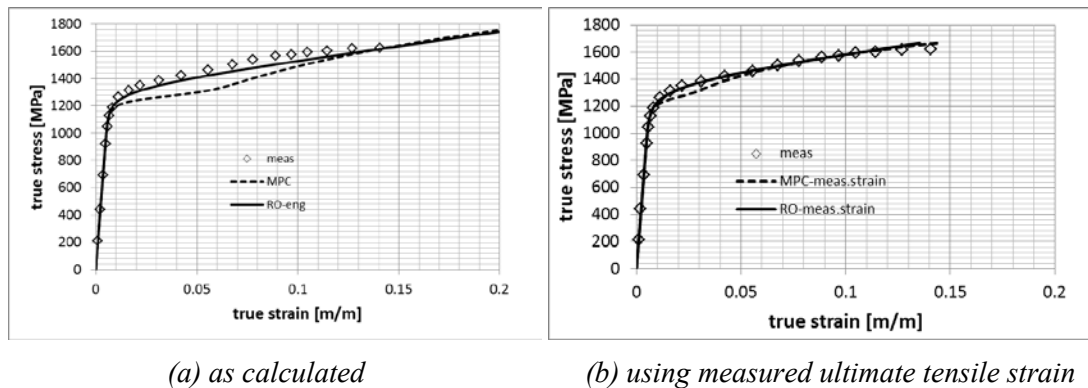


Figure 20—Comparison of Measured and Calculated Stress-strain Curves of IN-718 at Room Temperature

In Figure 20 the results using calculated ultimate tensile strain values are compared with results using the measured ultimate tensile strain. Figure 20 compares different approaches with measured data. MPC is the result of an application of the current MPC-procedure together with the m_2 -value given for gamma prime hardening alloys. RO-eng is the result of the RO-eng approach using the previously described third order polynomial for the determination of the ultimate tensile strain. Both approaches predict much too high ultimate tensile strains and consequently much too high true ultimate tensile stresses. Whereas for the MPC-approach also the shape of the curve differs significantly from the experimental values can the RO-eng approach much better predict the measured shape. Interesting is the outcome when instead of the calculated ultimate tensile strain the actually measured ultimate tensile strain is used (MPC meas.-strain, RO-eng meas.-strain). With this input the experimental curve can be very well predicted.

4.6 Other Classes of Materials

Other material classes like Cu, Ti, Zr or Al show usually a power law dependence for the engineering stress-strain curves. Most differences come from differences between measured and predicted ultimate tensile strains. Particularly titanium alloys show sometimes only small differences between YS and UTS which can make troubles for the m_2 -determination (see Table 2).

Appendix C shows a variety of examples how the current MPC-method and the RO-eng method can predict experimentally determined stress-strain curves and tangent moduli from yield stress and ultimate tensile stress. A clear disadvantage of the current MPC approach is the discontinuity at the point where the slopes of the two power laws change. It has currently also no option built into to account for special effects like Lueders strains. It is therefore proposed to use the RO-eng approach for further code related procedures.

5 TANGENT MODULUS

The tangent modulus gives the slopes of the true stress-strain curves. It is therefore the first derivative of the true stress-strain curve. It can be derived either by numeric differentiation of the true stress strain curve or—when the analytic form of the curve is available—by simple calculation of the first derivative. In case of the MPC approach the formula is given in Sect. VIII/2 as shown in Figure 21.

$$E_t = \frac{\partial \sigma_t}{\partial \varepsilon_t} = \left(\frac{\partial \varepsilon_t}{\partial \sigma_t} \right)^{-1} = \left(\frac{1}{E_y} + D_1 + D_2 + D_3 + D_4 \right)^{-1} \quad (3.D.16)$$

where

$$D_1 = \frac{\sigma_t^{\left(\frac{1}{m_1}-1\right)}}{2m_1 A_1^{\left(\frac{1}{m_1}\right)}} \quad (3.D.17)$$

$$D_2 = -\frac{1}{2} \left(\frac{1}{A_1^{\left(\frac{1}{m_1}\right)}} \right) \cdot \left(\sigma_t^{\left(\frac{1}{m_1}\right)} \left\{ \frac{2}{K(\sigma_{uts} - \sigma_{ys})} \right\} \{1 - \tanh^2[H]\} + \frac{1}{m_1} \sigma_t^{\left(\frac{1}{m_1}-1\right)} \tanh[H] \right) \quad (3.D.18)$$

$$D_3 = \frac{\sigma_t^{\left(\frac{1}{m_2}-1\right)}}{2m_2 A_2^{\left(\frac{1}{m_2}\right)}} \quad (3.D.19)$$

$$D_4 = \frac{1}{2} \left(\frac{1}{A_2^{\left(\frac{1}{m_2}\right)}} \right) \cdot \left(\sigma_t^{\left(\frac{1}{m_2}\right)} \left\{ \frac{2}{K(\sigma_{uts} - \sigma_{ys})} \right\} \{1 - \tanh^2[H]\} + \frac{1}{m_2} \sigma_t^{\left(\frac{1}{m_2}-1\right)} \tanh[H] \right) \quad (3.D.20)$$

Figure 21—Scheme for Determination of the Tangent Modulus According to the MPC Procedure Described in Section VIII/2

For the RO-eng approach the tangent modulus can be determined according to the following procedure using the notation e, s for engineering strain and stress and ε, σ for true strain and stress:

$$\frac{d\sigma}{d\varepsilon} = \frac{d(s(1+e))}{ds} \frac{ds}{d(\ln(1+e))} \quad (30)$$

With the expression for the RO-fit in the engineering stress-strain picture

$$e = \frac{s}{E} + 0.002 \left(\frac{s}{s_{0.2}} \right)^n \quad (31)$$

one obtains

$$\frac{d(s(1+e))}{ds} = 1 + \frac{2s}{E} + 0.002(n+1) \left(\frac{s}{s_{0.2}} \right)^n \quad (32)$$

And finally for the tangent modulus:

$$\frac{d\sigma}{d\varepsilon} = \frac{\left(1 + \frac{2s}{E} + 0.002(n+1)\left(\frac{s}{s_{0.2}}\right)^n\right) \cdot \left(1 + \frac{s}{E} + 0.002\left(\frac{s}{s_{0.2}}\right)^n\right)}{\left(\frac{1}{E} + n \cdot 0.002\left(\frac{s}{s_{0.2}}\right)^{n-1}\left(\frac{1}{s_{0.2}}\right)\right)} \quad (33)$$

With this expression the tangent modulus can be easily calculated once the engineering stress-strain curve is known. As in the RO-approach only one slope occurs where the curves of the tangent moduli do not show the discontinuity of the MPC approach when at the point of change between the two slopes which is shown in Figure 22 taking 2.25Cr-1Mo at room temperature as an example.

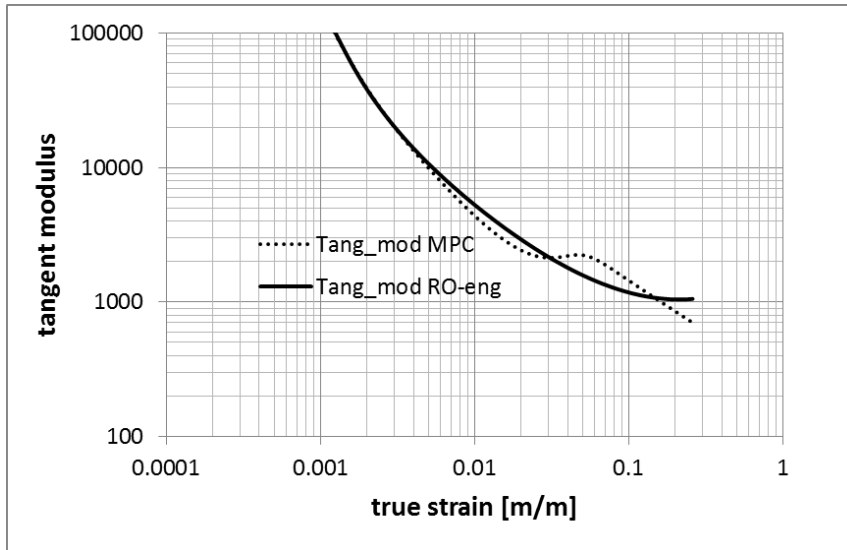


Figure 22—Comparison of Tangent Moduli Determined According to the MPC and to the RO-eng Procedure (Materials 2.25Cr-1Mo, RT)

It can be seen from this figure that except for the “jump” at slope change in the MPC representation the shape of the curve is very similar. More examples of tangent moduli can be found in Appendix C.

6 CYCLIC STRESS-STRAIN CURVES

Until now the discussion was limited to monotonic stress-strain curves. More complex is the field of fatigue curves or cyclic stress-strain curves. Basically, they are of same nature as tensile curves and they usually show a power law dependence. As typical low cycle fatigue deformations seldom exceed a total strain range of 1-2%, cyclic stress strain curves remain limited to the “low strain” regime and a one-power law approach can be used even for correlation between true cyclic strain and true cyclic stress. This procedure is used for determination of cyclic stress-strain curves in ASME VIII/2 according to the following formula:

$$\epsilon_{ta} = \frac{\sigma_a}{E_y} + \left[\frac{\sigma_a}{K_{css}} \right]^{\frac{1}{n_{css}}} \quad (34)$$

With total true strain amplitude, ϵ_{ta} , true stress amplitude, σ_a , Young’s modulus, E_y , and tabulated, materials dependent constants, K_{css} and n_{css} .

The main problem with cyclic stress-strain curves is that cyclic softening/hardening behavior of a material is currently unpredictable from materials data like yield stress, tensile stress or Young’s modulus with an engineering type of approach because it depends not only on the material but also on the condition of a material which shall be demonstrated with a simple example.

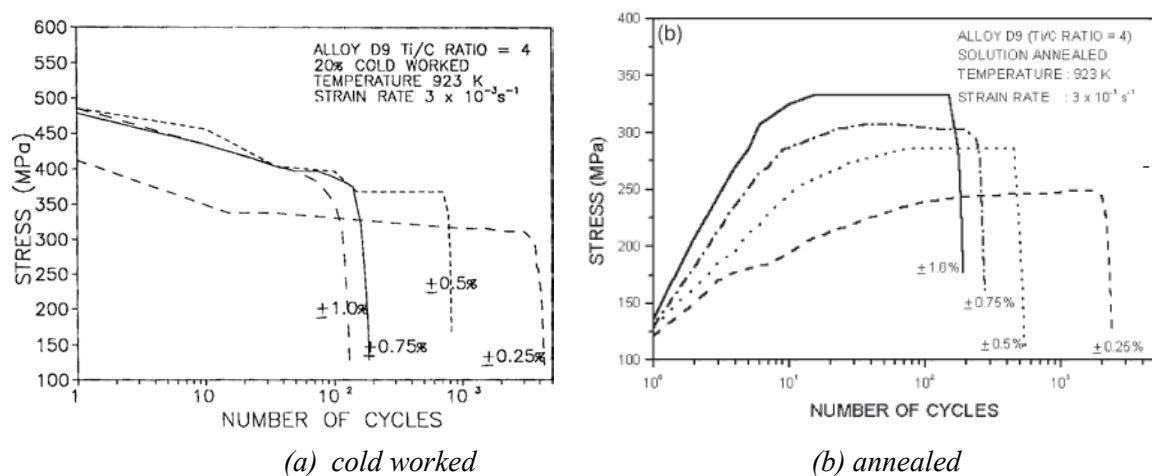


Figure 23—Cyclic Response of a Ti-containing Austenitic Steel at 650°C in 20% Cold Worked and in Annealed Condition [21]

Figure 23 shows the cyclic response of a Ti-containing austenitic steel at 650°C in 20% cold worked and in annealed condition. The cold worked material strongly cyclic softens, whereas the annealed quality strongly cyclic hardens. Although such behavior can be understood in terms of microstructure, it is currently impossible to quantify it in terms of stresses and strains without experiments. Cyclic stress-strain curves are usually determined at $\frac{1}{2}$ of the fatigue life which is on a logarithmic scale for number of cycles relatively close to the drop to final rupture. Cyclic stress-strain curves can be determined from different samples or with the so-called incremental step procedure where only one sample for which the stress is stepwise increased is used.

For code considerations it is important that cyclic stress-strain curves can only be established on the basis of existing experimental data. It is therefore anticipated that the cyclic stress-strain data given in Sect VIII/2 are based on measured data rather than on Y-1 and U-table values. Figure 24 shows a comparison of cyclic stress-strain curve for austenitic 304 steel published in the ASM-handbook [18]

with the curve determined for the same material under the same conditions in ASME VIII/2. A good agreement was found taking into consideration that the ASM-cyclic represents the measured curve whereas the ASME-curve is the result of equation 42.

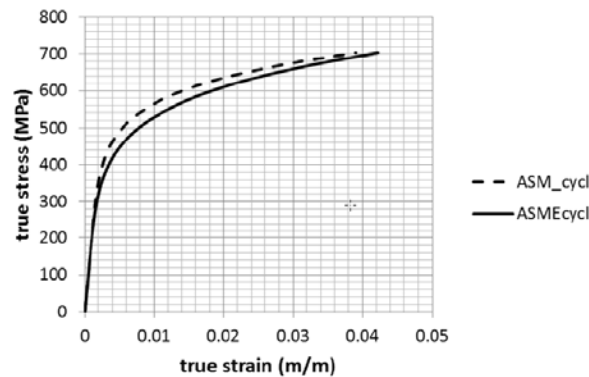


Figure 24—Comparison of Cyclic Stress-strain Curves for 304 at Room Temperature

In Figure 24, ASM_cycl represents the Data from the ASM handbook of stress-strain curves and ASMEcycl represents the curve which was calculated according to the ASME Code procedure.

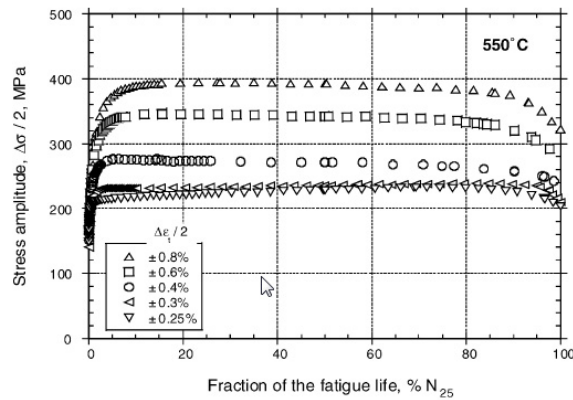
Possible procedures for the inclusion of new cyclic data into the code shall be discussed now. For this purpose it is important to notice that for many materials literature data exist which are usually given in form of the curves shown in Figure 23 and sometimes also cyclic stress-strain curves are given. But even when cyclic stress-strain curves are not given it is possible to construct cyclic stress-strain curves according to the procedure given in Appendix B as highlighted in the following with examples.

Figure 25 shows experimental results from LCF-tests of the austenitic steel 316LN in annealed condition [20]. From this figure stress amplitudes and total strain amplitudes for lowest and highest strain range can be determined at half-life. Under the assumption that these two points belong to a power law type stress-strain curve the full curve can be determined as shown in Figure 26a. The measured points refer to the measured cyclic stress-strain curve (which in this case was given in the paper together with the monotonic stress-strain curve as shown in Figure 26b). Taking the scatter of the experimental data into consideration an extremely good reproduction of the cyclic stress-strain curve was obtained with only two data points from the cyclic hardening curves.

The technically very important judgment if a material cyclic hardens or softens is only possible when both cyclic and monotonic stress-strain curves are known, which is the case for this demonstration example. But a procedure for introduction of cyclic stress-strain curves which is consistent with the Y-1 and U-tables is still missing and a pragmatic proposal for such a procedure will be given in the following.

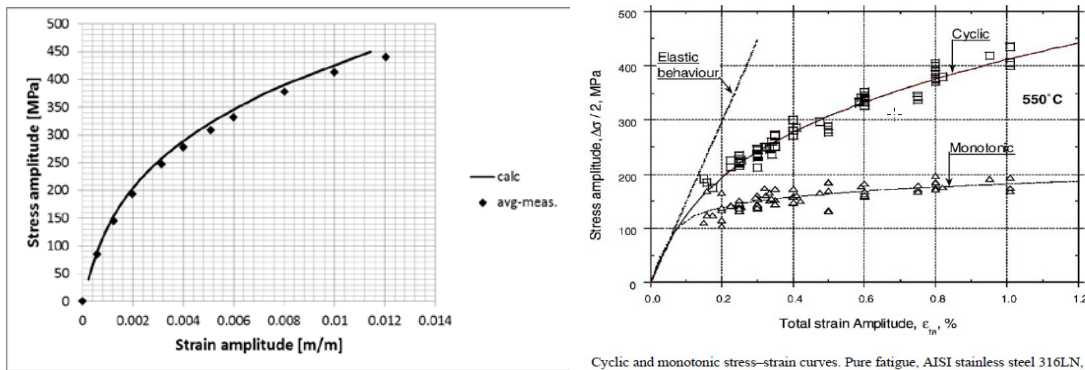
Steel 316 LN is also part of Y-1 and U-Tables and therefore the monotonic stress-strain curve according to the code can be obtained as previously discussed. This curve is considerably lower than the monotonic curve determined in the paper which can be seen from Figure 27a. “Experimental” refers in this figure to the published data (Figure 26b) and “Y-1/U” refers to the monotonic curve determined from Y-1 and U tables. If for future code developments a consistent set of cyclic stress-strain curves shall be established also scaling according to differences in monotonic curves becomes necessary. It is proposed to use the ratio between the yield stresses of the monotonic curves also for scaling of the cyclic curves. The results of such scaling are shown in Figure 27b. In this figure “cyclic-paper” refers to the published experimental data. “Cyclic_proposal” represents the cyclic stress-strain curve after scaling with the ratio of the monotonic yield stresses for possible introduction into a future code.

M. Sauzay et al. / Nuclear Engineering and Design 232 (2004) 219–236



Evolution of the stress amplitude with respect to the fraction of fatigue life. Pure fatigue, AISI stainless steel 316LN, 550 °C.

Figure 25—Experimental Results from LCF-tests of the Austenitic Steel 316LN in Annealed Condition [20]

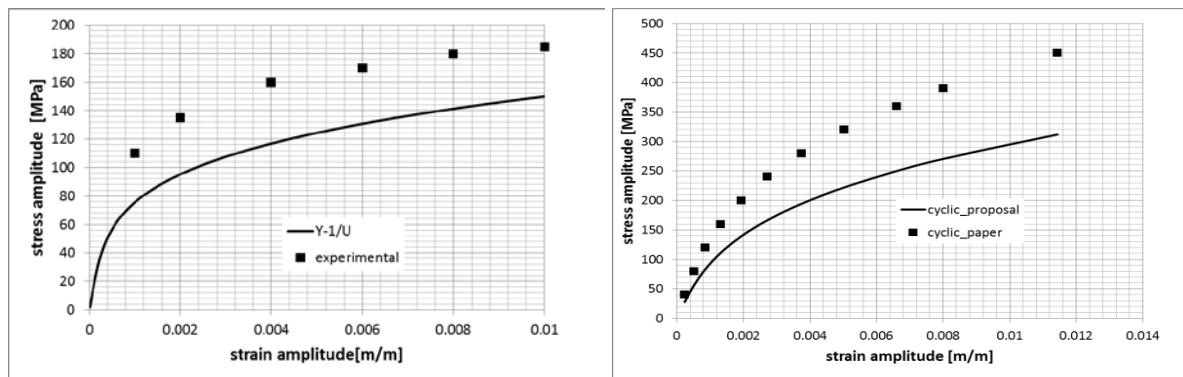


Cyclic and monotonic stress-strain curves. Pure fatigue, AISI stainless steel 316LN, 550 °C.

(a) Calculated cyclic stress-strain curve (b) Measured cyclic and monotonic stress-strain curves

Figure 26—Comparison of a Measured Cyclic Stress-strain Curve (b) with a Cyclic Stress-strain Curve Determined only from Two Data Points (a) Given in [20]

The monotonic stress-strain curve in (b) is considered for comparison with the monotonic stress-strain curve determined from Y-1/ Table values.



(a) Monotonic stress-strain curve from Fig 26(b) (b) Scaled cyclic stress strain curve

Figure 27—Proposal for Scaling of Cyclic Stress-strain Curve when Different Monotonic Curves Exist

For 316 LN the experimentally measured monotonic curve is considerably higher than the curve calculated from the Y-1/U Tables (a). For inclusion into the code this difference must be accounted for. It is proposed to use the ratio of the yield stresses for scaling – cyclic_proposal in (b).

High strength low alloy steel (HSLA) shall be taken as another example for conversion of literature data into cyclic stress-strain curves. Data for different HSLA steels were found in [22] for V, Cb and Ti-containing HSLA steels and in [23] for A-723 (SA-723). In both investigations monotonic stress-strain curves were found to follow very well to reasonably well a power law relation and comparable cyclic hardening was found. The literature data could be very well reproduced using the methods described above. Based on this information monotonic and cyclic stress-strain curves for different classes of SA-723 could be established using again the yield stress ratios for scaling. For the two extreme classes (Cl.1 and Cl.5) the results are shown in Figures 28a and b.

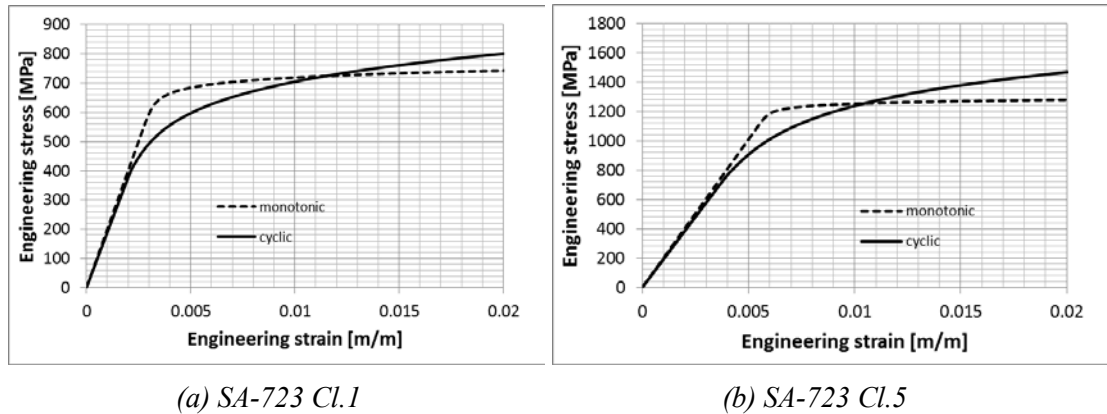


Figure 28—Monotonic and Cyclic Stress-strain Curves for Different Classes of SA-723 as Derived from Literature

Precipitation hardened austenitic steels of type 17-4 PH in qualities H900 and H1150 are considered as a final example for determination of cyclic stress-strain curves. The data were taken from an analysis of the fatigue behavior of notched samples [24]. To reconstruct the cyclic stress-strain curves the following procedure was chosen.

The fatigue curves were given in a Manson-Coffin representation (equ.35):

$$\varepsilon_a = \varepsilon_{ea} + \varepsilon_{pa} = \frac{\sigma_f'}{E} (2N_f)^b + \varepsilon_f' (2N_f)^c \quad (35)$$

The different coefficients and exponents were given in the paper which allowed the determination of the total stress amplitude, ε_a . The stress amplitude could be determined according to:

$$\sigma_{\max} \varepsilon_a = 36.0(N_f)^{-0.236} \quad (36)$$

This was found in [24] as the best correlation between number of cycles to failure and stress/strain amplitudes for several samples and several mean loads. For zero mean stress is σ_{\max} equal to σ_a and therefore the cyclic stress-strain curve is fully determined. Since also yield stress, ultimate tensile stress and Young's modulus have been given for the different qualities it was possible to determine also the monotonic stress-strain curve with the RO-eng method. The results of this analysis are shown in Figure 29 a,b for the qualities H900 and H1050. The dashed lines represent the monotonic curves as calculated according to RO-eng. For determination of

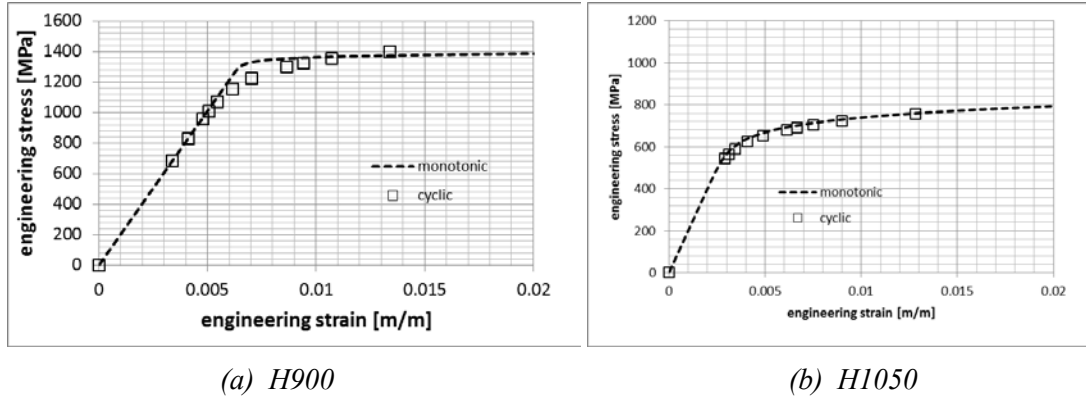


Figure 29—Cyclic and Monotonic Stress-strain Curves of 17-4 PH in Two Different Qualities

the squared points equations 43 and 44 were solved for different values on N_f . In good approximation it can be concluded that for 17-4 PH, the cyclic and monotonic stress-strain curves can be considered to be the same (at least for these qualities).

In many cases monotonic stress-strain curves and cyclic stress-strain curves are not available for the same material which can lead to confusion and errors concerning cyclic hardening/softening of materials as highlighted with an example from the current code edition. As an example, 9Cr-1Mo (grade 91) which is known as a cyclic softening martensitic steel was chosen.

It is included in the cyclic stress-strain curves of Sect. VIII/2 and it is also included in the Japanese NIMS database [25]. Figure 30a compares the cyclic stress-strain curve from NIMS and the cyclic stress-strain curve from ASME VIII/2 and an almost perfect agreement between those two curves can be seen. However, comparing the monotonic curves based on YS and UTS values given for this material in NIMS [25] and in Y-1-U-Tables, respectively a pronounced difference exists (Figure 30b).

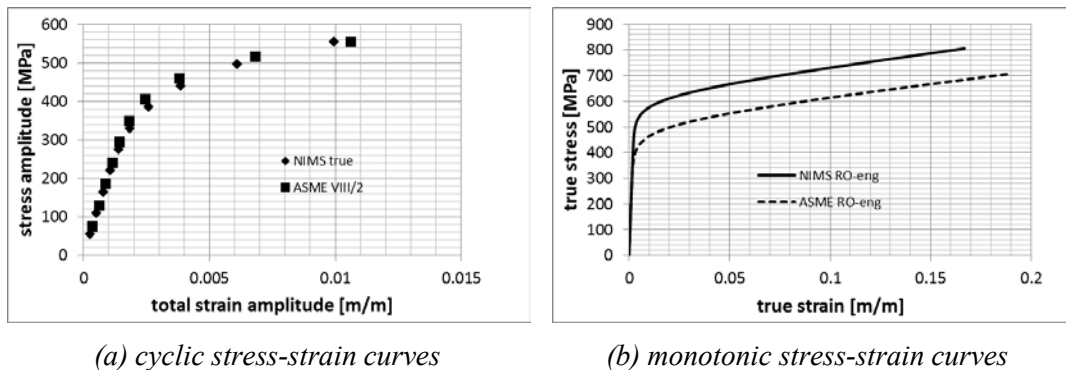
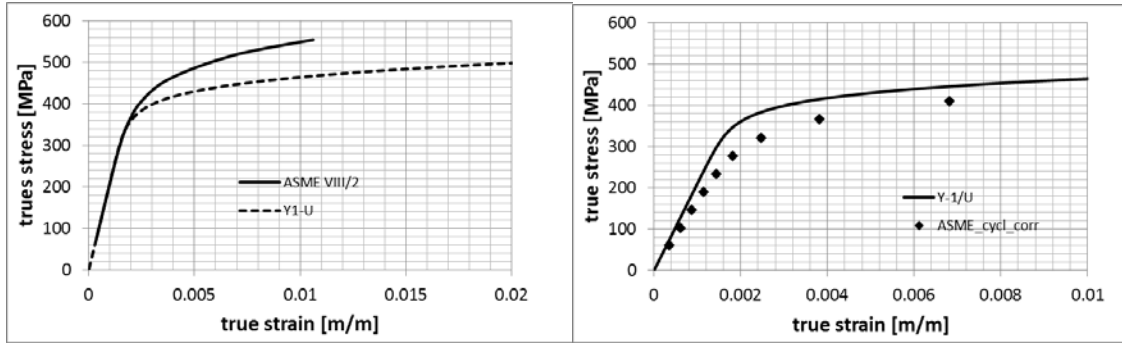


Figure 30—Cyclic and Monotonic Stress-strain Curves of Grade 91 Martensitic Steel According to the Japanese NIMS [25] Database and the ASME Code

In a next step the combination of monotonic curve and cyclic curve according to the code is shown in Figure 31a. From this figure the material is expected to be clearly cyclic hardening which is not at all true! Correcting the cyclic curve in the same way as previously discussed by the ratio between the yield stresses the cyclic curve shows clear cyclic softening, in agreement with NIMS [25] and the other literature.



(a) Current situation in the ASME-code (b) After scaling of cyclic stress-strain curve

Figure 31—Comparison of Cyclic and Monotonic Stress-strain Curves for Grade 91 in Current Code Edition

Without scaling, the material is expected to cyclic harden (Figure 31a). With yield-stress scaling, the expected (cyclic softening) behavior of the material is obtained.

Detailed knowledge about the cyclic stress-strain curve is important for fracture mechanics considerations like determination of the cyclic J-integral for fatigue crack growth which needs the hysteresis loop and determined the driving force of fatigue cracks in the LCF regime. Hysteresis loops are usually determined by scaling the cyclic stress-strain function by a factor of 2 which corresponds to the determination of the cyclic stress strain curves. With the notation of equation 42 the hysteresis loop can be determined according to equation 37:

$$\epsilon_r = \frac{\sigma_r}{E_y} + 2 \left[\frac{\sigma_r}{2K_{cy}} \right]^{\frac{1}{n_{cy}}} \tag{37}$$

Summarizing, it can be stated that for cyclic stress-strain curves the shape is no problem, because for several materials a power law relationship is found and complications like Lueders strain do not exist. The real uncertainty concerns the cyclic hardening/softening behavior which is almost unpredictable and which can only be determined with experimental results. But even then a careful adjustment between cyclic and monotonic curves has to be made to get consistent code entries. To provide sound solutions for these issues it is recommended that further research based on existing data and literature be performed.

7 PROPOSAL FOR IMPLEMENTATION OF STRESS-STRAIN CURVES INTO THE ASME CODE

It is an aim of further code editions to add monotonic and cyclic stress-strain curves and it was one aim of this study to analyze current procedures with respect to possible implementation.

Currently most widely used in the code is the MPC-approach which is a two power law approximation of the true stress strain curve using only Y-1 Table and U-Table values for reconstruction of the true stress-strain curve. Additional data like the expected ultimate tensile strain (m_2) and strain when first plasticity occurs (ϵ_p) are available as materials dependent tabulated values. This is a sound procedure which has certainly its merits but also its limitations (discontinuities when switching from low strain to high strain regime, inaccurate ultimate strain values, etc.).

Besides this method also a one-power law parameterization for the true stress strain curve (called Ramberg Osgood in the code) is in use. This designation is not quite correct because Ramberg-Osgood developed their parameterization for engineering stress-strain curves, not for true stress-strain curves. It was Hollomon [3] who proposed a power law fit of the true stress-strain curve. Simple mathematic considerations reveal that due to the nature of the definition of true stress and true strain a one power law fit of the true stress-strain curve will fail even if the engineering stress-strain curves can be very well described with one power law relation.

For the determination of isochronous stress-strain curves in Sect III, a polynomial fit is employed for the determination of stress-strain curves.

An amended procedure shall:

- Give (where possible) more accurate results as the current procedures
- Allow constructing stress-strain-curves from Y-1 and U-Table values
- Lead to results which allow maintaining existing data and procedures as much as possible
- Be simple and straightforward in its application.

Based on analyses of experimental data and comparisons of different approaches the following procedure for determination of stress-strain curves (engineering and true) is proposed:

Determine the engineering stress-strain (e-s) curve according to

$$e = \frac{s}{E} + 0.002 \left(\frac{s}{s_{YS}} \right)^n$$

with s_{YS} = yield stress according to Y-1 Table, Young's modulus, E.

The exponent n is calculated according to:

$$n = \log \left(\left(e_{UTS} - \frac{s_{UTS}}{E} \right) / 0.002 \right) / \log (s_{UTS} / s_{YS})$$

with s_{UTS} = StRt (U-table value corrected by 1.1) and e_{UTS} = ultimate tensile strain determined from Δs which is the difference between $s_{UTS} - s_{YS}$ by:

$$e_{UTS} = 1.1903E-08. \Delta s^3 - 5.687E-06. \Delta s^2 + 1.847E-3. \Delta s$$

Determine the true stress-strain curve according to the well-known procedure:

$$\varepsilon = \ln(1+e) \text{ and } \sigma = s(1+e)$$

Determine tangent modulus according to:

$$\frac{d\sigma}{d\varepsilon} = \frac{\left(1 + \frac{2s}{E} + 0.002(n+1)\left(\frac{s}{s_{0.2}}\right)^n\right) \cdot \left(1 + \frac{s}{E} + 0.002\left(\frac{s}{s_{0.2}}\right)^n\right)}{\left(\frac{1}{E} + n \cdot 0.002\left(\frac{s}{s_{0.2}}\right)^{n-1}\left(\frac{1}{s_{0.2}}\right)\right)}$$

Comments:

- This procedure covers the wide range of materials for which the engineering stress-strain curve follows a power law relationship. This is no restriction in comparison with the current code procedures which are also based on this assumption.
- Most uncertainties are in the determination of e_{UTS} which needs further analysis based on more experimental data. The third order potential proposed here gives reasonable results which are comparable with the Sect VIII/2 m_2 values.
- For materials where e_{UTS} is known this value shall be used instead of the 3rd order polynomial.
- Lueders-strains which often occur for low carbon steels can be included into the procedure.
- Secondary hardening effects (encountered e.g. for austenitic steels at temperatures below room temperature and other occasionally occurring effects, e.g. pronounced upper and lower yield strength) cannot be accounted for. It is recommended to cover such materials and material conditions with experimental data.
- Inclusion into the current stress tables can be done simply by reference to YS and UTS and a set of notes referring to the above mentioned comments.
- The attached Excel-map (Appendix D) allows determination of such curves including the option of entering the measured UT-strain and a Lueders-strain.

Although cyclic stress-strain curves usually follow a power law relationship its determination cannot be based on YS and UTS because of the strong influence of material and materials conditions on the cyclic hardening/softening behavior. Already existing cyclic stress strain curves in the code appear to be based on experimental results. Although for the small strains which are usually considered for cyclic stress-strain curves also the true stress-strain curves can be described by a simple power law it is recommended to start also the cyclic stress-strain curves from the engineering picture. Many cyclic data are available in the open literature and in databases like the Japanese NIMS [25] database and could be used to establish more cyclic stress-strain curves.

As usually total strain amplitudes and stress amplitudes are reported it is possible to determine the cyclic stress strain curves according to:

$$e_a = \frac{s_a}{E} + A\left(\frac{s_a}{s_i}\right)^n$$

with the strain amplitude, e_a , the stress amplitude, s_a and a normalizing stress, s_i .

Pick two appropriate pairs of total strain amplitudes and total stress amplitudes from a typical LCF-investigation: (e_1, s_1) and (e_2, s_2) and take e.g. s_1 as normalizing stress. The equation above can then be written as:

$$\frac{s_1}{E} + e_{1,pl} = \frac{s_1}{E} + A \left(\frac{s_1}{s_1} \right)^n$$

with $e_{1,pl}$ being the plastic part of e_1 which can always be determined from total strain and Young's modulus.

One obtains:

$$A = e_{1,pl}$$

And for n one calculates

$$n = \frac{\lg \left(\frac{e_2 - \frac{s_2}{E}}{e_{1,pl}} \right)}{\lg \left(\frac{s_2}{s_1} \right)}$$

which defines the required stress-strain curve.

It is important to point to the fact that for inclusion of cyclic curves into the code a consistency between monotonic curves and cyclic curves must be given. It is therefore proposed to scale curves from different investigations with the ratio of the yield stresses.

Hysteresis loops can be conveniently constructed by scaling the cyclic stress-strain curves with a factor of two. Effects like the Bauschinger effect are not covered this way which seems to be acceptable in the same way as also for monotonic curves no differentiation between tensile and compression curves is made.

8 REFERENCES

- [1] W. Ramberg and W. Osgood, Description of Stress-strain Curves by Three Parameters, National Advisory Committee for Aeronautics, TN 902, 1943.
- [2] K. Samuel and P. Rodriguez, On Power-law Type Relationships and the Ludwigion Explanation for the Stress-strain Behavior of AISI 316 Stainless Steel, *J. Materials Science*, 40, pp. 5727–5731, 2005.
- [3] H. Hollomon, *Trans. AIME*, 162, p. 268, 1945.
- [4] P. Arasaratnam, K. Sivakumaran and M. Tait, True Stress-True Strain Models for Structural Steel Elements, International Scholarly Research Network ISRN Civil Engineering, vol. 2011, Article ID 656401, 2011.
- [5] K. Singh, Strain Hardening Behavior of 316L Austenitic Stainless Steel, *Materials Science and Technology*, vol. 20, Sept. 2004.
- [6] R. Swindeman, Isochronous Stress vs. Strain Curves for Normalized-and-tempered 2 1/4 Cr-1 Mo Steel, ASME Pressure Vessel and Piping Conference, Orlando, FL., July 27-31, 1997.
- [7] J. Hammond and V. Sikka, Predicted Strains in Austenitic Stainless Steels at Stresses above Yield, Effects of Melting and Processing Variables on the Mechanical Properties of Steel, MPC-6, ASME, New York, pp. 309-322, 1977.
- [8] N. Cofie, G. Miessi and A. Deardorff, Stress-strain Parameters in Elastic-Plastic Fracture Mechanics
- [9] A. Olsson, Stainless-steel Plasticity, Doctoral Thesis, University of Lulea, 2001.
- [10] A. Bowen and P. Partridge, Limitations of the Hollomon Strain-hardening Equation, *J. Phys. D: Appl. Phys.*, vol. 7, pp. 969-978, 1974.
- [11] H. Kleemola and M. Nieminen, On the Strain-hardening Parameters of Metals, *Metallurgical Trans.*, vol. 5, p. 1863, Aug. 1974.
- [12] P. Ludwik, *Elemente der Technologischen Mechanik*, Verlag von Julius Springer, Berlin, 1909.
- [13] H. Swift, *J. Mech. Phys. Solids*, vol. 1, pp. 1-18, 1952.
- [14] R. Blandford, D. Morton, S. Snow and T. Rahl, Tensile Stress-strain Results for 304L and 316L Stainless Steel Plate at Temperature, ASME Pressure Vessels and Piping Division Conference, July 2007, INL/CON-06-11962.
- [15] B. Hantz, private communication, March 2012.
- [16] K. Rasmussen, Full-range Stress-strain Curves for Stainless Steel Alloys, Research Report R811, University of Sidney, 2001.
- [17] R. Brockenbrough, Properties of Structural Steels and Effects of Steelmaking and Fabrication, *Structural Steel Designer's Handbook 4th ed.*, McGraw Hill, New York.
- [18] ASM-Atlas of Stress-strain Curves, 2nd ed., ASM, 2002.
- [19] R. Swindeman, Isochronous Stress vs. Strain Curves for Normalized-and-tempered 2 1/4 Cr-1 Mo Steel, ASME Pressure Vessel and Piping Conference, Orlando, Florida, July 27-31, 1997.

- [20] M. Sauzay et al, Creep-fatigue Behavior of an AISI Stainless Steel at 550°C, Nuclear Engineering and Design 232, pp. 219–236, 2004.
- [21] R. Sandhya et al, Substructural Recovery in a Cold Worked Ti-modified Austenitic Steel During High Temperature Low Cycle Fatigue, Int. J. Fatigue 23, pp. 789-797, 2001.
- [22] A. Sherman, Fatigue Properties of High Strength Low Alloy Steels, Met. Trans A (1975) 6A, pp. 1035-1040, 1975.
- [23] E. Troiano, J. Underwood, D. Crayton and R. Abott, Low Cycle Fatigue Behavior and Life Predictions of A723 High Strength Steels, U.S. Army ARDEC Benet Laboratories, AMSTA-AR-CCB-O, Watervliet, NY, 1995.
- [24] Ch.-K. Lin and Ch.-Ch. Chu, Mean Stress Effects on Low-cycle Fatigue for a Precipitation Hardening Martensitic Stainless Steel, Fatigue Fract. Engng Mater Struct 23, pp. 545-553, 2007.
- [25] NIMS database, http://mits.nims.go.jp/index_en.html
- [26] J. Grubb ATI-metals, Private communication, June 2012.

APPENDIX A – DETERMINATION OF THE STRESS-STRAIN CURVE USING TWO DATA POINTS

Let us assume that the engineering stress-strain curve can be described with a Ramberg-Osgood relationship:

$$e = \frac{S}{E} + A \left(\frac{S}{S_i} \right)^n \quad (A.1)$$

with S , engineering stress, S_i , normalizing stress, e , engineering strain, E , Young's modulus, A and n , constants.

Assume two data points from a given engineering stress-strain curve: (e_1, S_1) and (e_2, S_2) and take e.g. S_1 as normalizing stress. Equation A.1 can then be written as:

$$\frac{S_1}{E} + e_{1,pl} = \frac{S_1}{E} + A \left(\frac{S_1}{S_1} \right)^n \quad (A.2)$$

with $e_{1,pl}$ being the plastic part of e_1 .

And one obtains:

$$A = e_{1,pl} \quad (A.3)$$

Using the second point gives:

$$e_2 = \frac{S_2}{E} + e_{1,pl} \left(\frac{S_2}{S_1} \right)^n \quad (A.4)$$

After some rearrangement one gets:

$$n = \frac{\lg \left(\frac{e_2 - \frac{S_2}{E}}{e_{1,pl}} \right)}{\lg \left(\frac{S_2}{S_1} \right)} \quad (A.5)$$

The shape of the curve is now fully described by A and n given in equations (A.3) and (A.5). From this curve usually $\sigma_{0.2}$ can be easily determined.

Determination of the Ultimate Tensile Stress (UTS):

The UTS cannot be easily determined from the stress-strain curve. One possibility offers the Considère plot in which the true stress is plotted as a function of the engineering strain as shown in Figure 32.

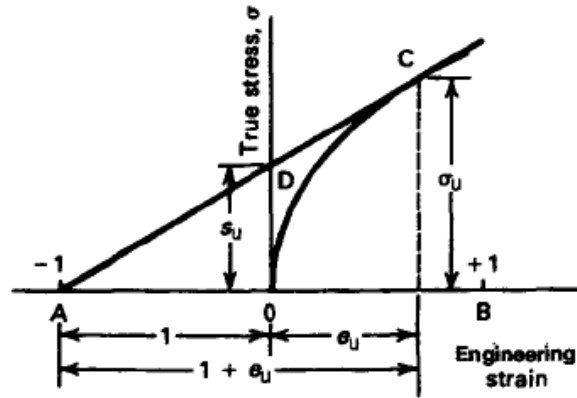


Figure 32—Considère Plot for the Determination of the Maximum Stress (UTS)

Based on different trials with existing curves it could be shown that the curve 0-C can be very well approximated by a power law:

$$\sigma_i = B e_i^\beta \quad (\text{A.6})$$

with σ_i , true stress at point i , e_i , engineering strain at point i and B , β , constants. With two points from the curve 0-C (σ_1 , e_1 and σ_2 , e_2) the constants can be easily calculated according to the relations (A.7) and (A.8):

$$\beta = \frac{\lg\left(\frac{\sigma_2}{\sigma_1}\right)}{\lg\left(\frac{e_2}{e_1}\right)} \quad (\text{A.7})$$

and

$$B = \frac{\sigma_1}{e_1^\beta} \quad (\text{A.8})$$

We therefore obtain

$$\sigma_{UTS} = B e_{UTS}^\beta \quad (\text{A.9})$$

The second condition comes from the fact that the line -1-C is a tangent to the curve 0-C at point C. This leads to the relation

$$\frac{d\sigma}{de} \Big|_{UTS} = B\beta e_{UTS}^{\beta-1} = \frac{\sigma_{UTS}}{1 + e_{UTS}} \quad (\text{A.10})$$

From which we calculate

$$\beta = e_{UTS} + e_{UTS}^2 \quad \text{which is in good approximation } e_{UTS} \quad (\text{A.11})$$

Together with relation (9) σ_{UTS} and e_{UTS} can be calculated.

This leads to the following general procedure for reconstruction of a full range stress-strain curve.

1. Obtain a given stress-strain curve as data points (either experimental values or after digitization).
2. Determine A and n according to equations A.3 and A.5 which defines the curve in terms of a Ramberg-Osgood parametrization.
3. Determine the yield stress as the intersection of the curve $\epsilon_{pl} = A \left(\frac{\sigma}{S_t} \right)^n$ with the line $\epsilon_{pl}=0.002$.
4. Convert the Ramberg-Osgood curve from an e-s into an e- σ -representation using equations A.6, A.7, A.8.
5. Determine ϵ_{UTS} according to A.8, A.9, A.10 and A.11.
6. Determine the standardized form of the Ramberg-Osgood curve based on 0.2 pct yield strength and ultimate tensile stress.
7. Determine the true stress-strain curve according to the standard procedure described in the main part of the paper.

Although this looks like a very complicated procedure it is extremely straightforward and it can be conveniently performed as an Excel-based procedure.

This procedure was applied to a set of published engineering stress-strain curves of 2 ¼ Cr-1Mo measured at different temperatures.

APPENDIX B – COMPARISON FOR IN 800H (RATIONAL POLYNOMIAL, ASME II, RAMBERG-OSGOOD)

Figure 33 compares the polynomial fit from the Task 13 report with a recently discussed Ramberg-Osgood type power law fit which is also exclusively based on YS and UTS. It is currently considered as one option to determine ASME stress-strain curves from Y-1 and U-Table values.

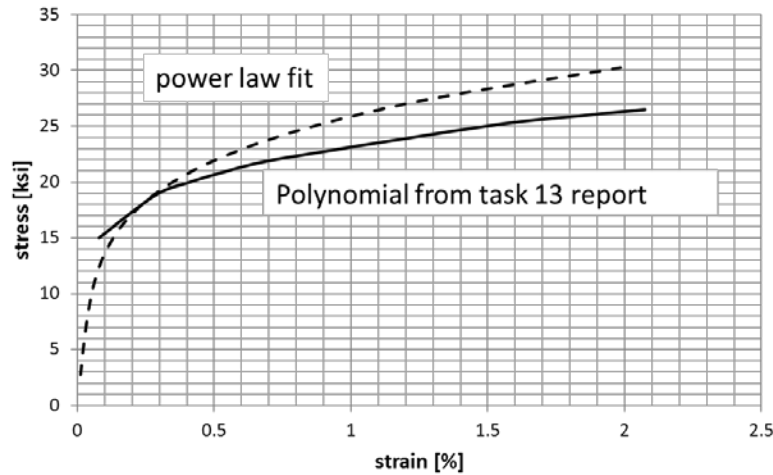


Figure 33—Comparison of the Polynomial Fit with a YS and UTS Based Power Law Fit

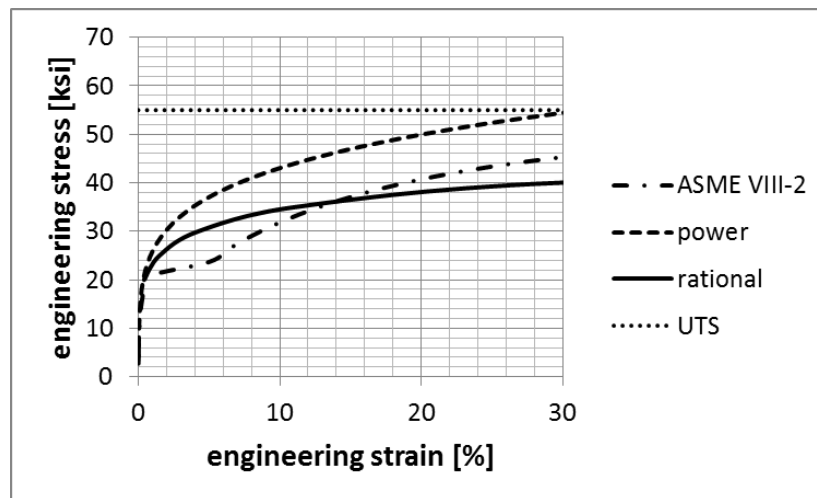


Figure 34—Comparison of Different Parameterizations of Stress-strain Curves Applied to IN 800H Determined at 1100F

Figure 33 shows that there is a discrepancy between the two fitting techniques. However, one could argue that the polynomial fit must be valid only at rather small strains whereas the power law fit should cover the whole range up to UTS. And from that point of view one could even state that the agreement is not too bad. However, finally the curves must meet the UTS at reasonable strains (expectedly 10-30%) which should also be reflected in the slope. The more global perspective can be seen in Figure 34. The curve compares the fitting of the rational (taken from the Task 13 report) with the fit of the results of the current ASME-VIII-2 stress-strain curve fitting and a Ramberg-Osgood type fitting (called power in Figures 33 and 34). Also ASME VIII-2 and power are exclusively based on YS and UTS. The very important information concerns the UTS which is indicated as dotted line and which must be finally reached by several approaches. In this frame the power law fit shows a

very appropriate appearance in contrast to the polynomial fit. For further clarification the German KTA-rules were considered in accordance with the Task 13 report. The analyses were performed with data representing 900°C which are shown in Figure 35. The 0.01h curve was chosen as representative (like in the Task 13 report). This curve was digitized and the points taken are shown in Figure 36.

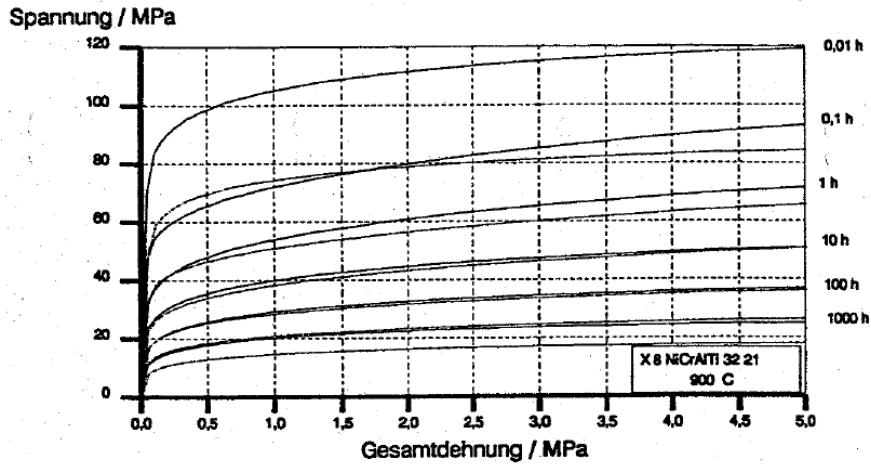


Figure 35—Isochronous Stress-strain Curves from the German KTA

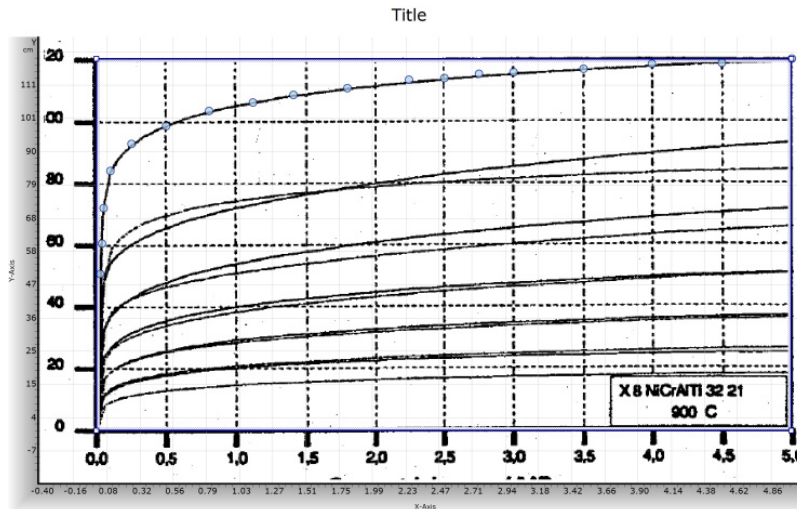


Figure 36—Identification of the Points Taken for Digitization of the KTA Stress-strain Curve

This curve was now compared with the results gained from the power law parametrization using exclusively YS and UTS (mean values) given in the KTA. The result is shown in Figures 37 and 38 which are comparable to Figure 33 and 34.

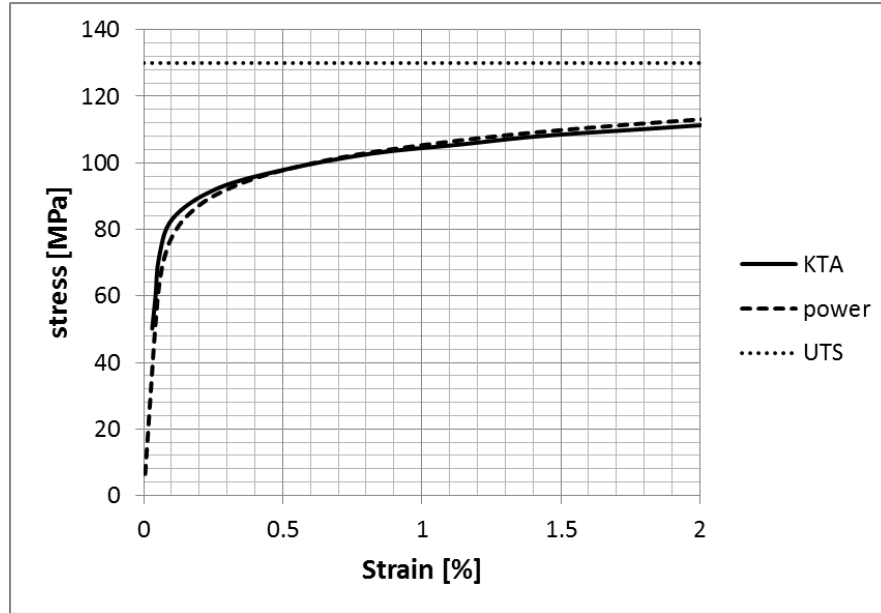


Figure 37—Comparison of YS-UTS Based Power Law Fit with KTA-data at Low Strains

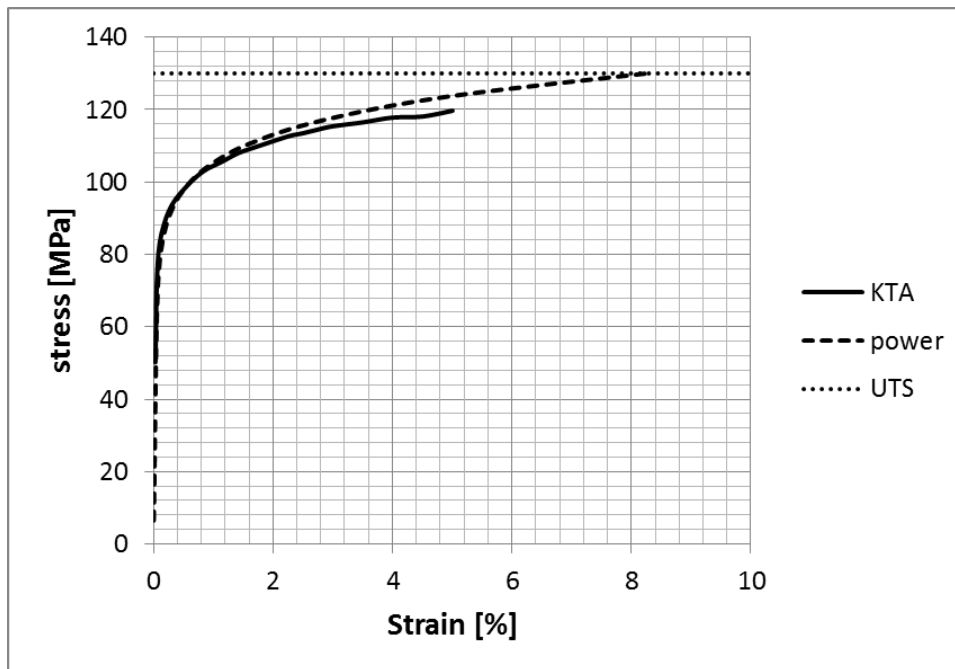


Figure 38—Comparison of YS-UTS Based Power Law Fit with KTA-data at High Strains

In the low strain regime an almost perfect agreement was found. And also in the high strain regime the data agree quite well. The differences are mainly determined by the choice of the UT-strain used for the power law. In this analysis the UT-strain was determined from the $(UTS-YS)/E$ which turned out to give reasonably good assessments. The two curves also meet the UTS in the expected range. In the KTA also the plastic strains are shown (see Figure 39). These plastic strains were compared with the plastic strains determined with the power law fit described above. The agreement is surprisingly good.

Temperatur (C)	900									
Dehnung (%)	0,001	0,010	0,050	0,100	0,200	0,500	1,000	2,000	5,000	
Zeit (h)	0,01	54	66	79	85	91	98	105	111	120

Figure 39—Plastic Strains for the Stress-Strain Curves Determined in KTA.

Legend: Dehnung/plastic strain, Zeit (h) means basically time, but the values refer to the stress (in MPa) corresponding to the respective plastic strains.

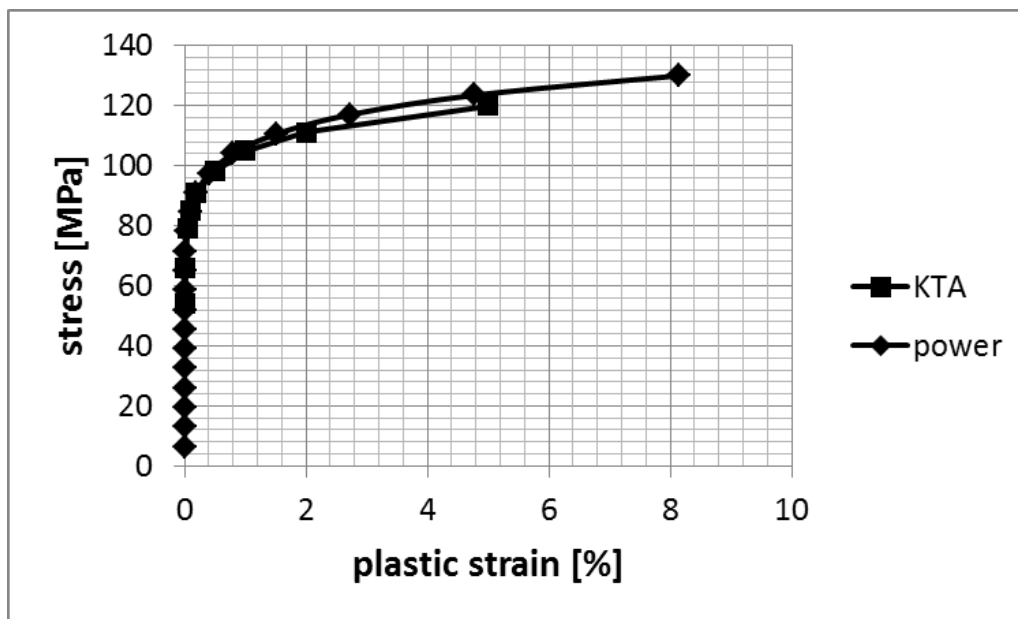
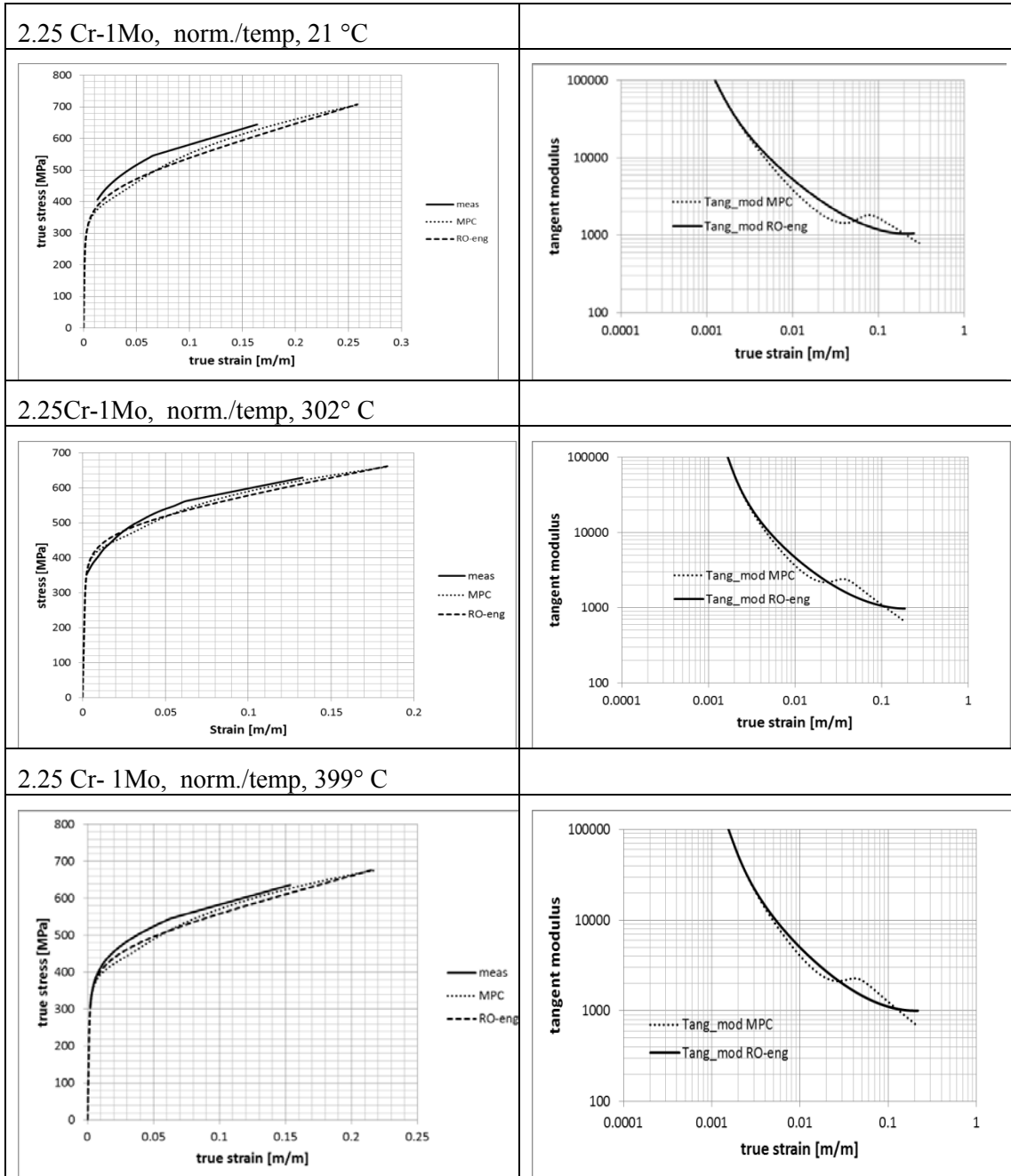


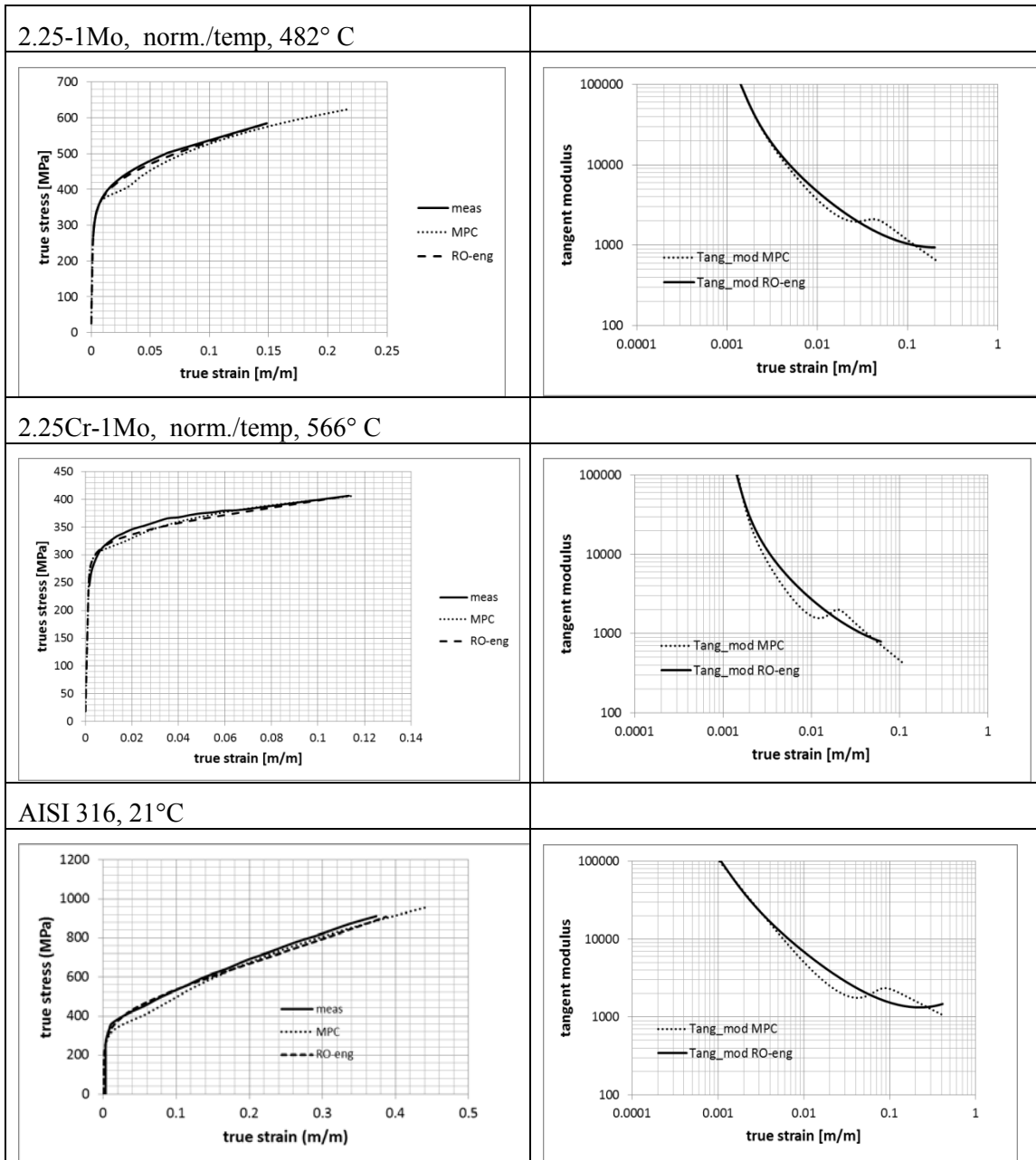
Figure 40—Comparison of Plastic Strains Taken from Figure 39 with the Ones Determined with the Power Law Fit Procedure

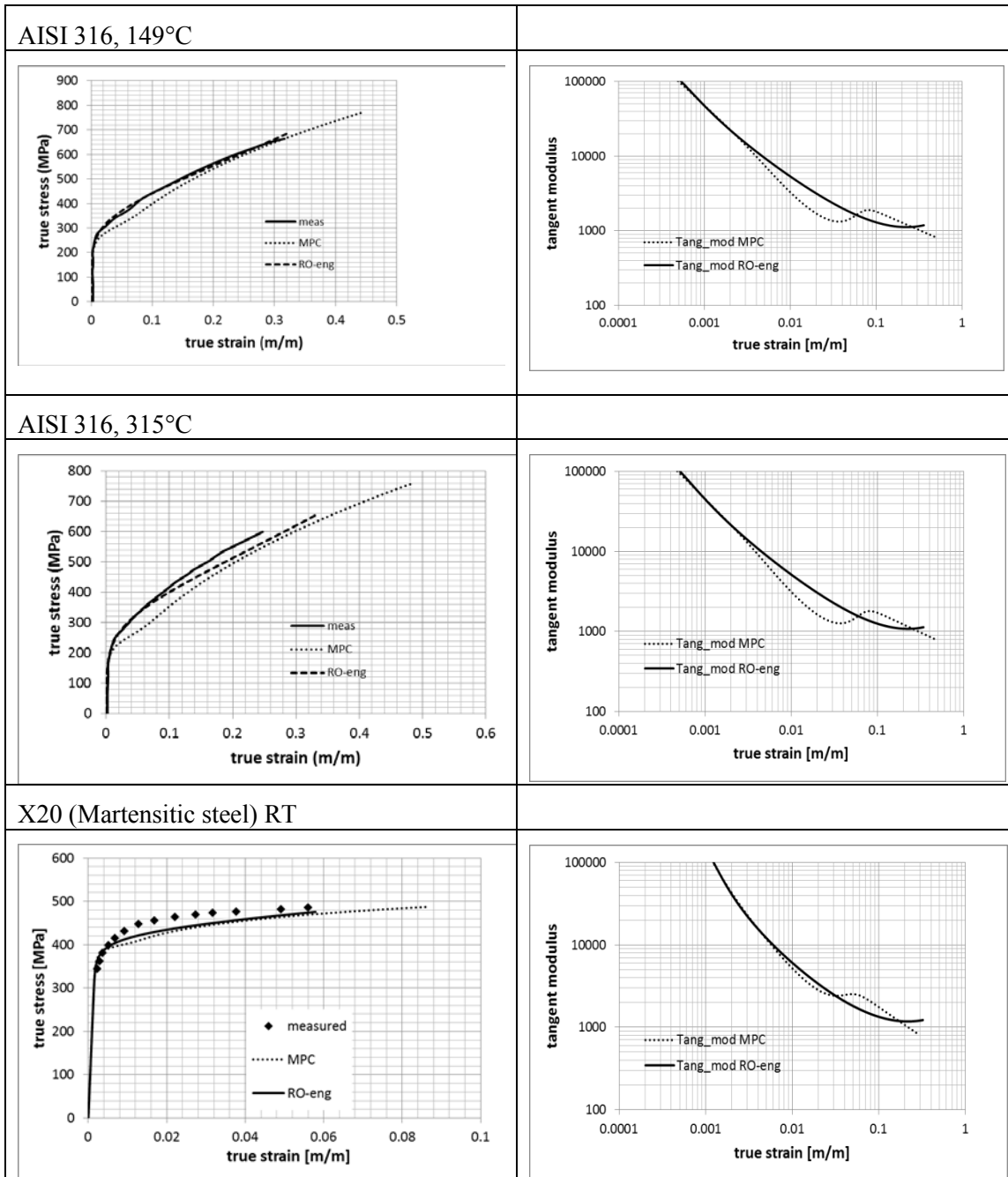
Conclusions:

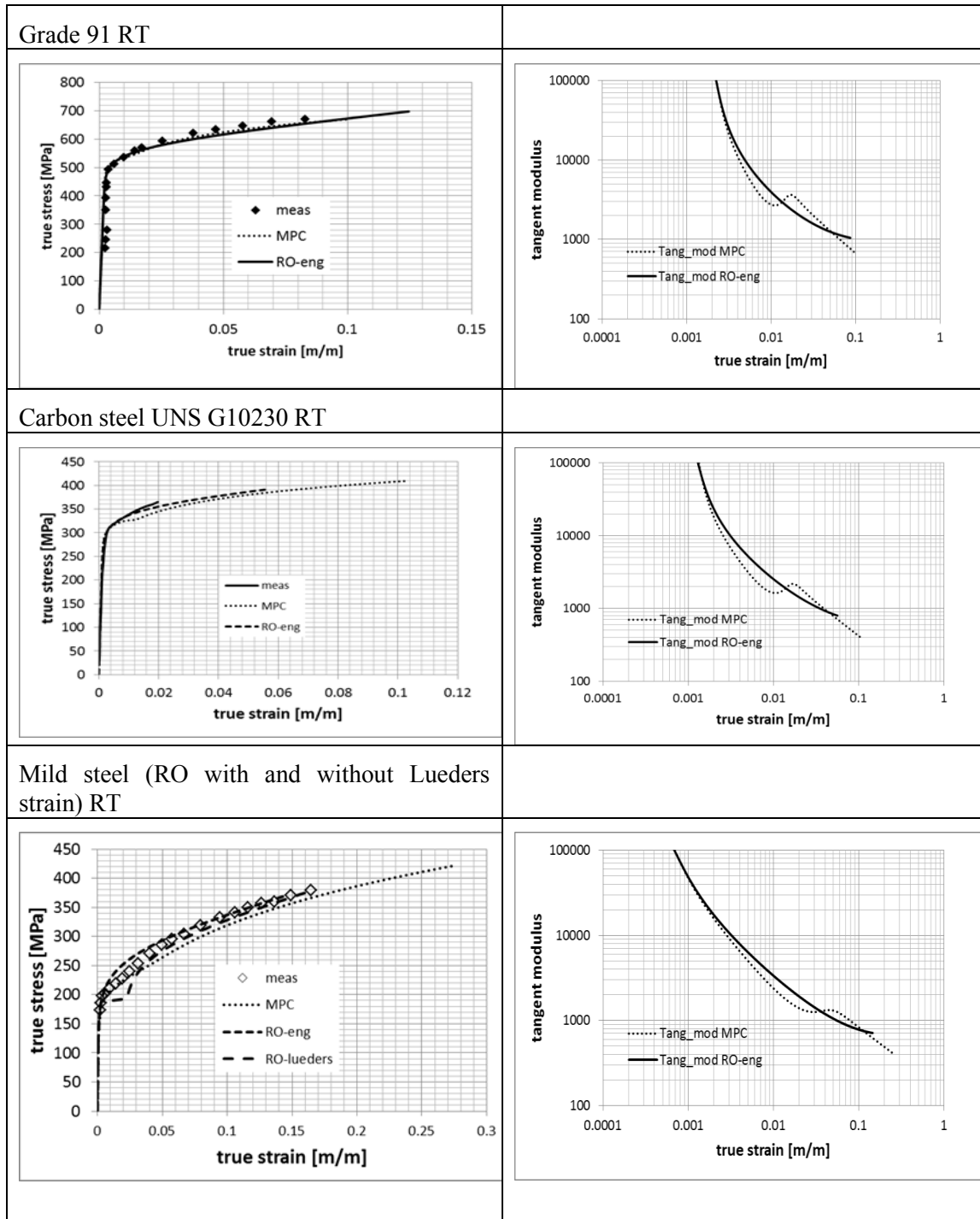
- The polynomial fit for the stress-strain curves presented in the task 13 report are certainly in good agreement with NH-curves.
- However, it looks like the determined slopes would not account properly for the UTS.
- A Ramberg-Osgood type power law fit only reasonably well agrees with the polynomial fit for NH, however it better accounts for the UTS.
- In contrast to this, the power law fit showed an excellent representation of the old KTA-curves at 900°C.
- It is therefore impossible to judge about the capability of the different fitting procedures
- It would be interesting to make the comparison with a set of experimental data which have not already been biased by code related smoothing exercises like for NH or KTA.
- The results of such a comparison could be used for eventual reconsideration of the NH stress-strain curves.

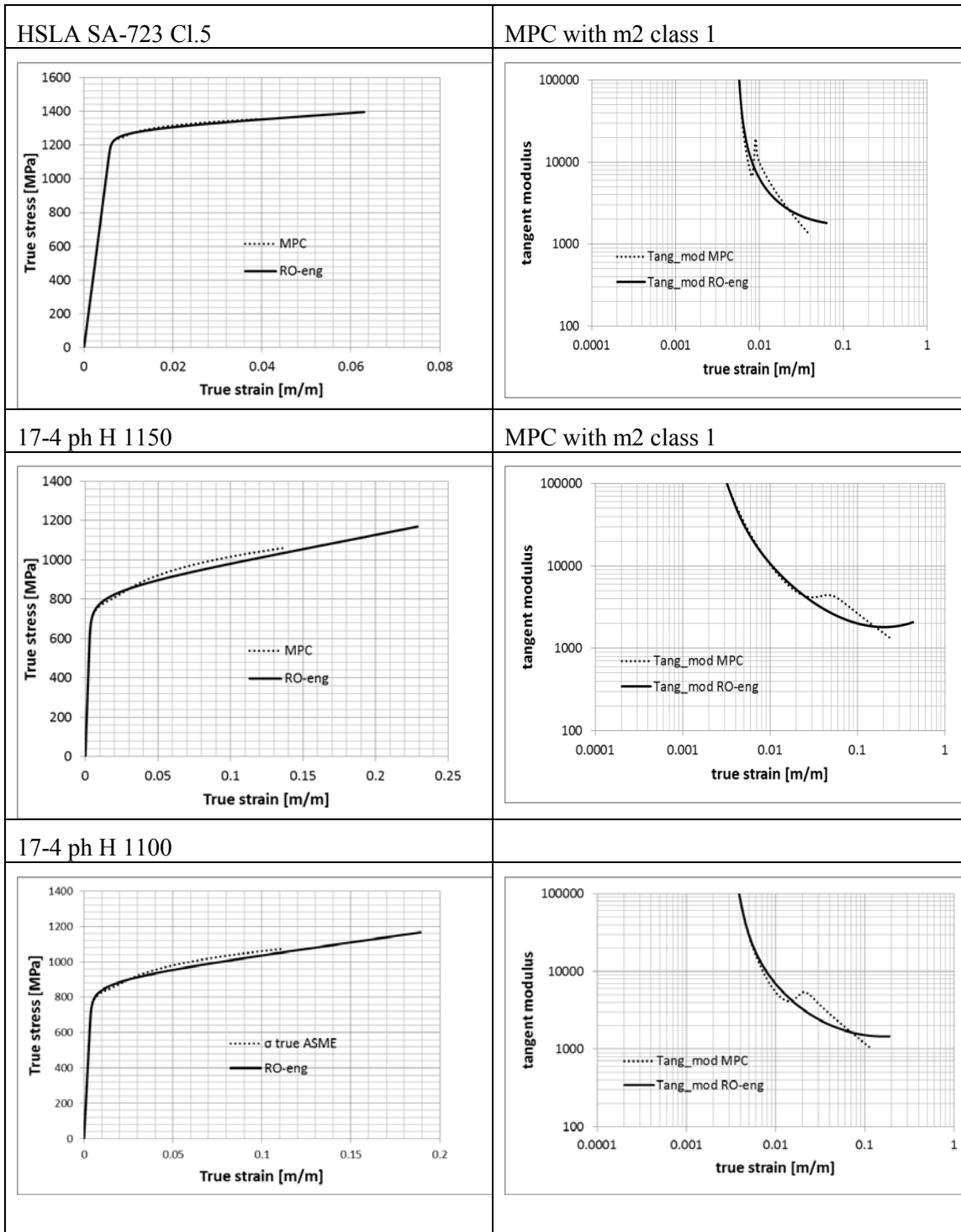
**APPENDIX C – DATA-SHEETS (TRUE STRESS-STRAIN CURVES, MODULUS)
FOR CROSS COMPARISON**

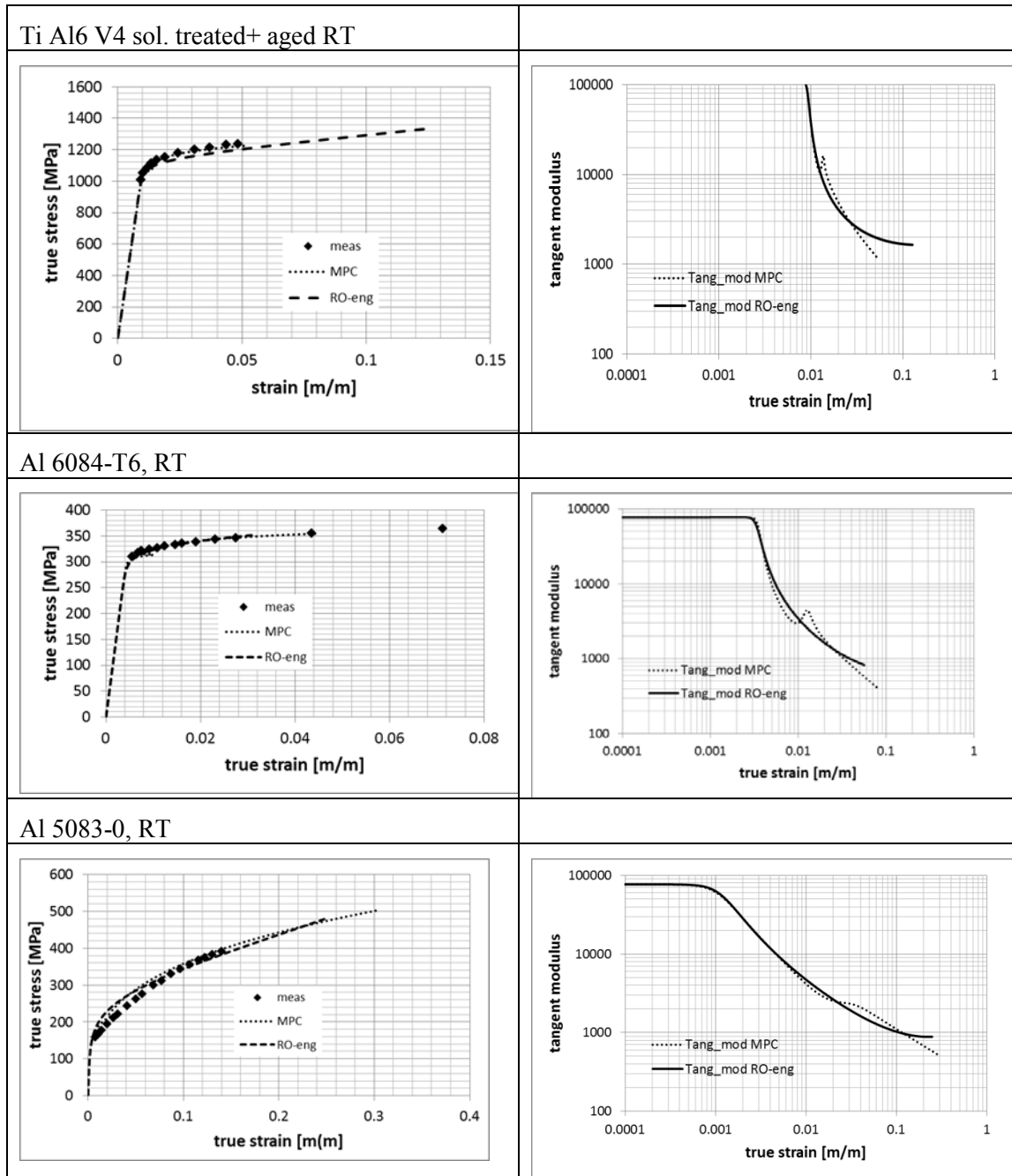


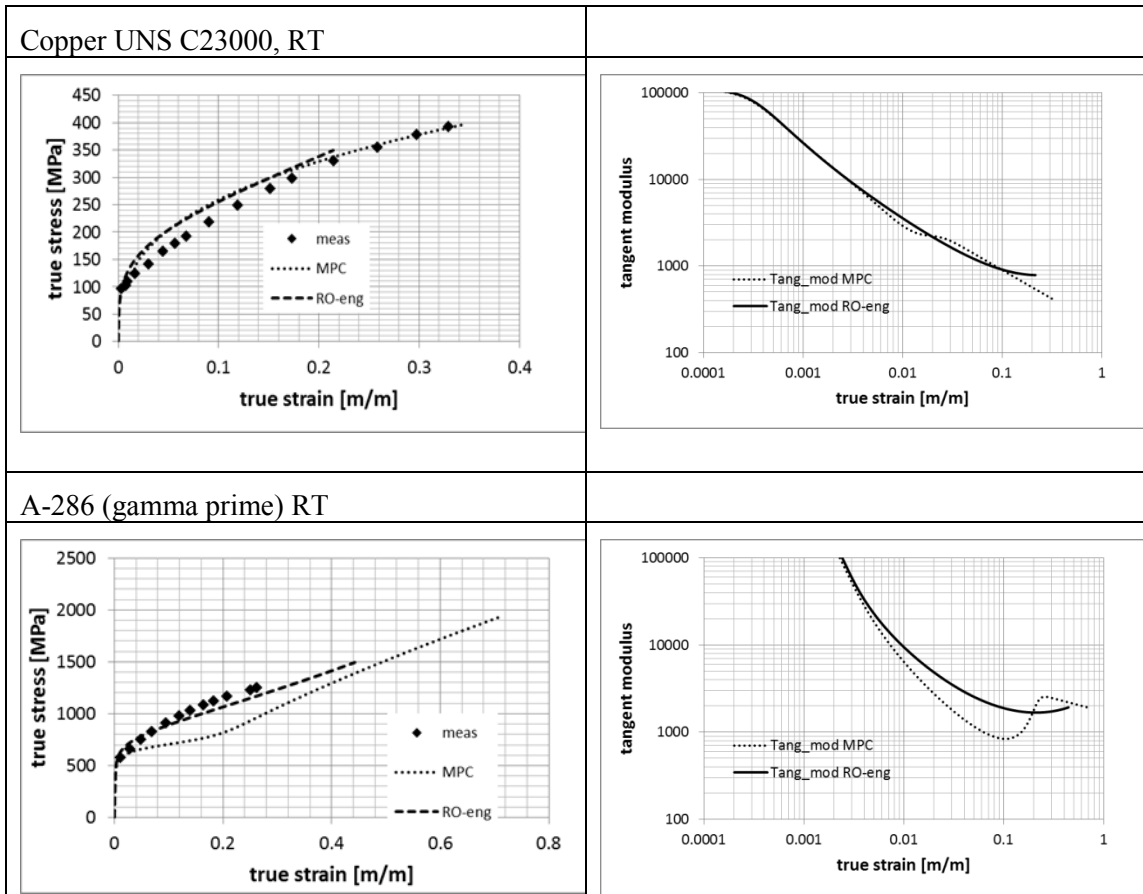






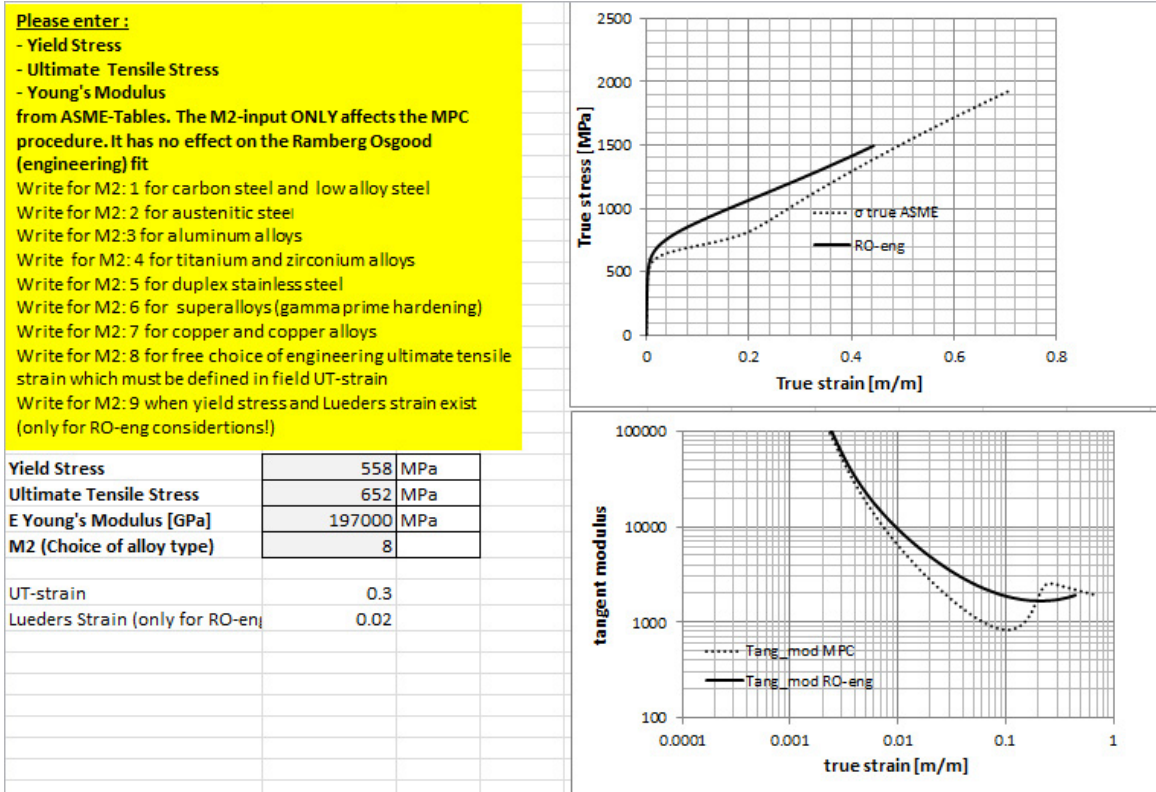






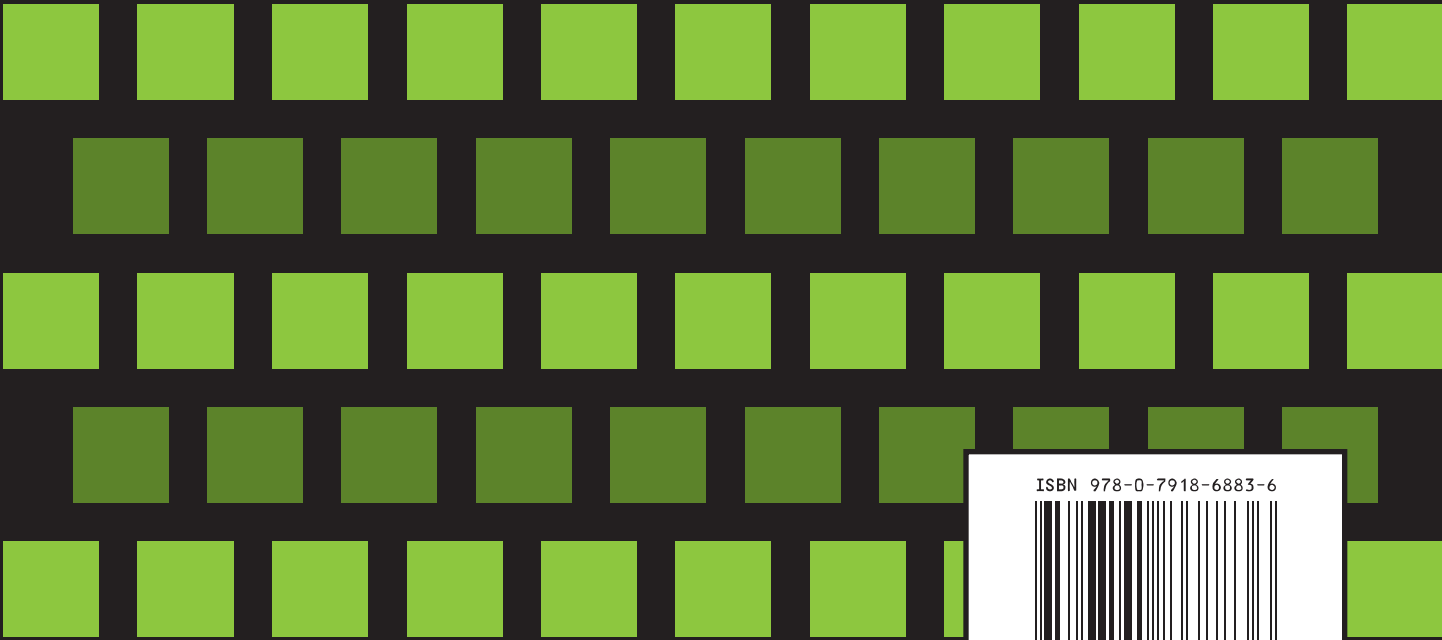
APPENDIX D – EXCEL MAP WHICH CALCULATES STRESS-STRAIN CURVES AND TANGENT MODULI ACCORDING TO MPC AND RO-ENG

Optionally experimentally determined ultimate tensile strain or Lueders strain can be inserted. For each curve 200 data points are calculated.

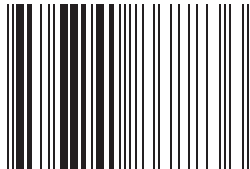


ACKNOWLEDGMENTS

The author acknowledges, with deep appreciation, the activities of ASME ST-LLC and ASME staff and volunteers who have provided valuable technical input, advice and assistance with review of, commenting on, and editing of, this document.



ISBN 978-0-7918-6883-6



9 780791 868836



A2421Q